Geological Survey Paper 11:

Structural Geology of the Eastern Southern Tyennan Domain, Tasmania

Author: D. R. Gray and M. J. Vicary
Date: 13/10/2022
Email: info@mrt.tas.gov.au
Website: www.mrt.tas.gov.au

REPORT No.: GSP11

Cover description: View of the southwest-closing isoclinal macro-fold in the northern face of Harrys Bluff. The photo is taken from Mt Wilson looking to the southeast. The steeply dipping quartzite in the left foreground is on Mt Wilson with the Old River valley in between. The hinge of the macro-fold is plunging into the valley towards the camera. (Photo Credit: Rock Monkey Adventures)

Tasmanian Government
Mineral Resources Tasmania
mrt

Contents

Abstract

The eastern part of the Southern Tyennan domain covers an area of approximately 1200 km² with a width of ~20 km and length of ~60 km and occupies almost one third of the Southern Tyennan region. It consists of a ~2 km composite metamorphic sheet made up, from top to base, of obducted platy quartzite, quartzite, low-grade pelite and high-grade schist. The outcrop pattern and structural formlines in So/Sm and Sm define an ovoid form, also expressed in the topography, with a broad, box-like fold geometry that has ~45 km width. This feature is the result of fold interference between early 2nd order macro-isoclines and younger Devonian north-south trending, east-west trending and northwest-trending open folds.

Structurally the eastern Southern Tyennan domain consists of three orders of macro-isoclinal folds including 1) northern termination of the South West Cape mega-fold system as a refolded 1st order downward-closing fold-nappe with an approximate axial surface length of 30 km, 2) 2nd order macro-folds that fold quartzite-pelite units within the hinge of the 1st order fold-nappe and the Red Point macro-fold folding high-grade schist and pelite with wavelengths of ~5 km, and 3) 3rd order macro-fold pairs with wavelengths of ~400-500 m that define a regional "wave train" above a high-strain lower bounding zone.

The 2nd order macro-folds include the Mt Robinson, Mt Braddon and Red Point macro-folds. The downward-closing Mt Robinson and Mt Braddon folds are approximately symmetrical W- folds within the plunging nose (la tete plongee) of the South West Cape mega-sheath fold system. The fold-nappe nose shows a reversal in unit stacking from the upper limb to the lower limb.

The 3rd order folds in the inferred fold "wave train" consist of repeated S-vergent, asymmetric fold pairs. The fold pairs have a limb separation distance (equivalent fold wavelength) of ~400-500 m, an upper-hinge to lower-hinge separation distance of ~400-450 m. At Harrys Bluff the fold pair can be seen in the quartzite cliffs, where the quartzite unit thickness is ~700 m. A series of structural profiles across the region of the "wave train" demonstrate the continuity of the asymmetric fold pair and their apparent occurrence at the same structural level. The fold-pair 1) sits structurally below the South West Cape mega-sheath fold system, but may also be a lateral transition away from the plunging nose with the Crossing Plains and Mt Braddon macro-isoclinal folds, and 2) occurs within the mega-sheath fold lower limb in the quartzite-dominated sequences. The quartzite shows a high strain transition towards a contact with a low-grade pelite sequence of dolomite and dolomitic phyllite. The pelite sequence occupies the Solly River Valley, the Crest Range, Forest Hills and Provis Hills in the far eastern part of the Southern Tyennan domain. It is the structurally lowest unit of the Southern Tyennan domain and is equated with the para-autochthonous dolomitic phyllite of the Scotchfire metamorphic sheet in the Central Tyennan domain (see Gray and Vicary, 2021a, b).

Tasmanian Government

Mineral Resources Tasmania

Department of State Growth
www.mrt.tas.gov.au

Structural Geology of the Eastern Southern Tyennan Domain, Tasmania

David R. Gray[1] and Michael J. Vicary[2]
[1] *Consultant Structural Geologist to Mineral Resources Tasmania*
[2] *Geological Survey Branch - Mineral Resources Tasmania*

ARTICLE INFO

Published: 13 October 2022
Publisher: Mineral Resources Tasmania
Report No.: GSP11

KEYWORDS

Structural Geology
Macro-isoclinal folds
Southern Tyennan

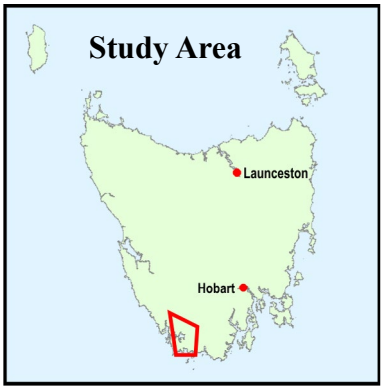

1.0 INTRODUCTION

The Southern Tyennan domain consists of several major and distinct structural entities (Figure 1) that are defined and discussed in a series of Tasmanian Geological Survey Papers. They include the high-grade south-west coastal belt (Gray et al, 2022) shown as elements 1 and 2 in Figure 1, the mega-sheath fold system core (Gray & Vicary, 2022b) shown as elements 3, 4 and 5 in Figure 1, with element 6 in Figure 1 as the eastern part dominated by an asymmetric, isoclinal macro-fold pair, including the easternmost Arthur Range (Gray & Vicary, 2022a) and finally element 7 in Figure 1 as the macro-structure of the Red Point metamorphic complex (Gray and Vicary, 2022c). This will be followed by a structural compilation and synopsis of the overall architecture of the Southern Tyennan domain (Gray and Vicary, 2022d).

The eastern part of the Southern Tyennan region, as described here, extends from Bathurst Harbour to the Eastern Arthur Range (Figures 2, 3 and 4). It covers an area of approximately 1200 km^2 with a width of ~20 km and length of ~60 km, approximately one third of the Southern Tyennan region.

Helicopter flights into the southwest on February 22, 2019 and March 26, 2020 provided glimpses of the overall structure of this part of the Southern Tyennan domain. En route into the area photographs taken every 30 seconds of the visible geology, combined with bushwalker photographs and the limited available structural data, enabled subsequent definition of the regional structure. Recumbent, tight to isoclinal, regional scale folds were seen in isolated hillside exposures throughout the area (Figures 5 and 6 as examples).

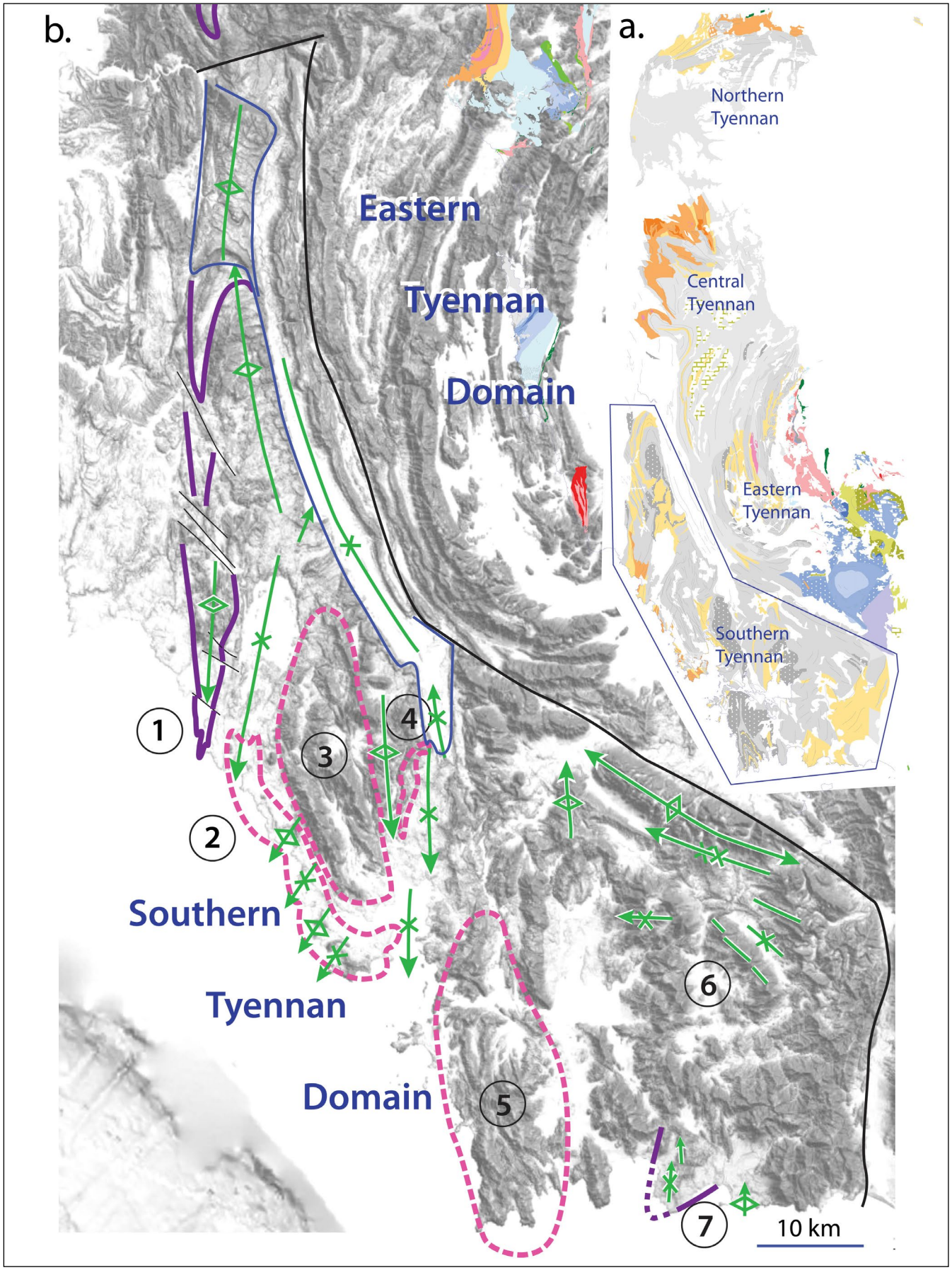

Figure 1. Major structural elements of the Southern Tyennan domain with ListMap greyscale digital elevation model as base map. Purple lines are So/Sm formlines that outline the Nye Bay-Charles Range fold-nappe (element 1) and the Red Point macro-fold (element 7). Pink dashed lines show the approximate extent and positions of the isoclinal fold stack (element 2) and the De Witt-Propsting mega-sheath fold (element 3), the Davey River sheath nose (element 4), the South West Cape mega-sheath (element 5). Element 6 represents the remaining area to the east as the isoclinal macro-fold domain. Element 7 is the Red Point isoclinal macro-fold, part of the isoclinal fold domain. The axial surface traces of younger, Devonian folds that fold the older Cambrian macro-structures are shown by the green line traces. The black solid line is the faulted boundary between the Southern and Eastern Tyennan domains. Rotating the map to the west west provides an oblique intersection through the Southern Tyennan crustal profile.

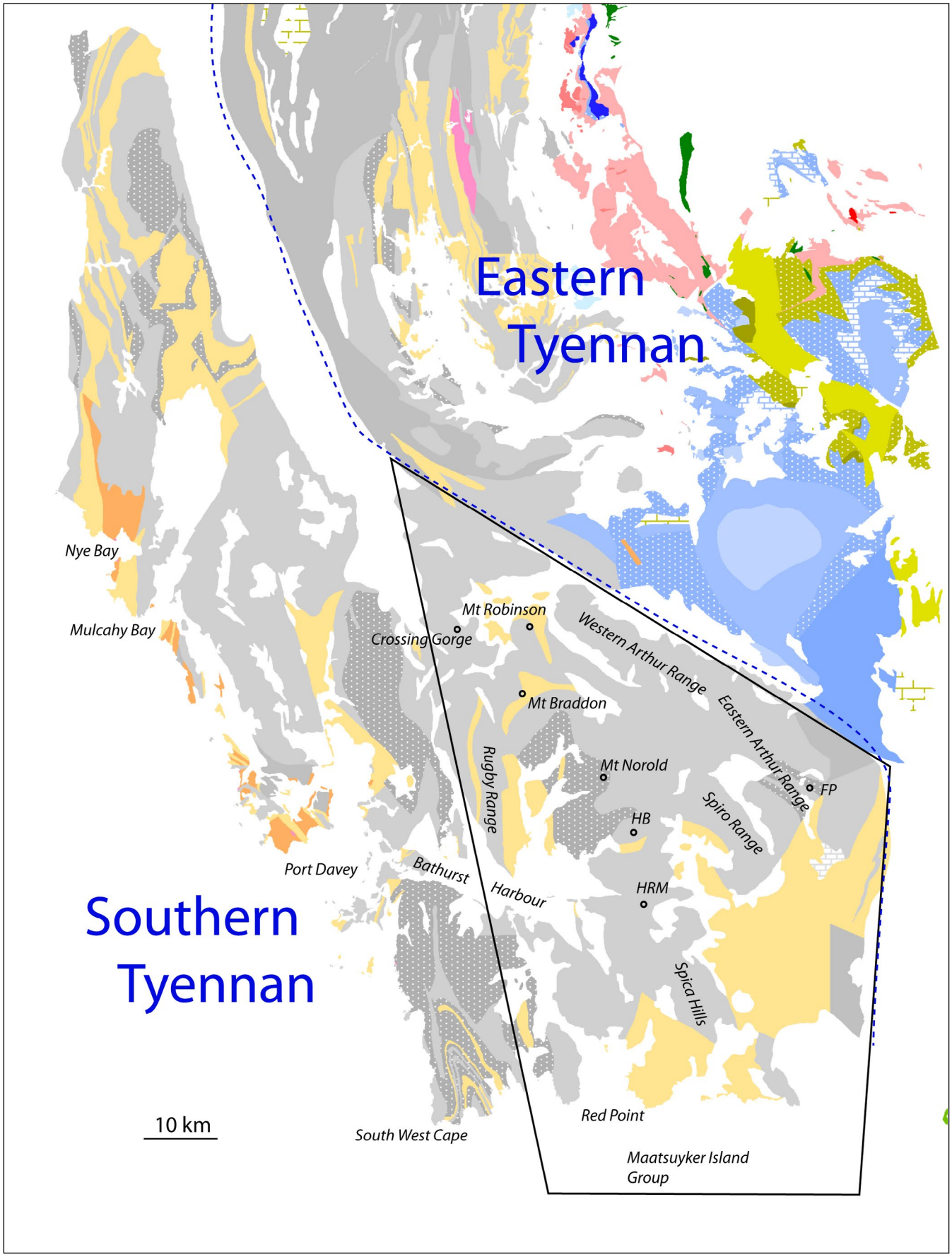

Figure 2. Geological map of the Southern and Eastern Tyennan domains with the eastern part of the Southern Tyennan domain, as discussed in this paper, shown by the black outlined polygon. The map base is from the Mineral Resources Tasmania 1:250000 digital geological Atlas. Geographic features include HB: Harrys Bluff. HRM: High Round Mountain. FP Federation Peak. The blue dashed line is the boundary between the Eastern and Southern Tyennan domains. The eastern Southern Tyennan map polygon base is 5165000N with eastern boundary 465000E and the top left corner 418800E, 5239400N.

Figure 3. ListMap Topographic map of the eastern part of the Southern Tyennan region. The region enclosed by the red dashed line extends from the Crossing River in the northwest to the Hopetoun Range in the northeast, to Mt Louisa and Louisa Plains in the southeast, to the Maatsuyker Island group in the south, with the approximate western boundary through the New Harbour Range northwards to the Rugby Range and Bakers Range. The northern flank of the Arthur Range defines the northeastern boundary. Topographically the curvature and orientation of these eastern ranges reflect interference between northwest-trending, north-trending and east-trending open, younger Devonian folds.

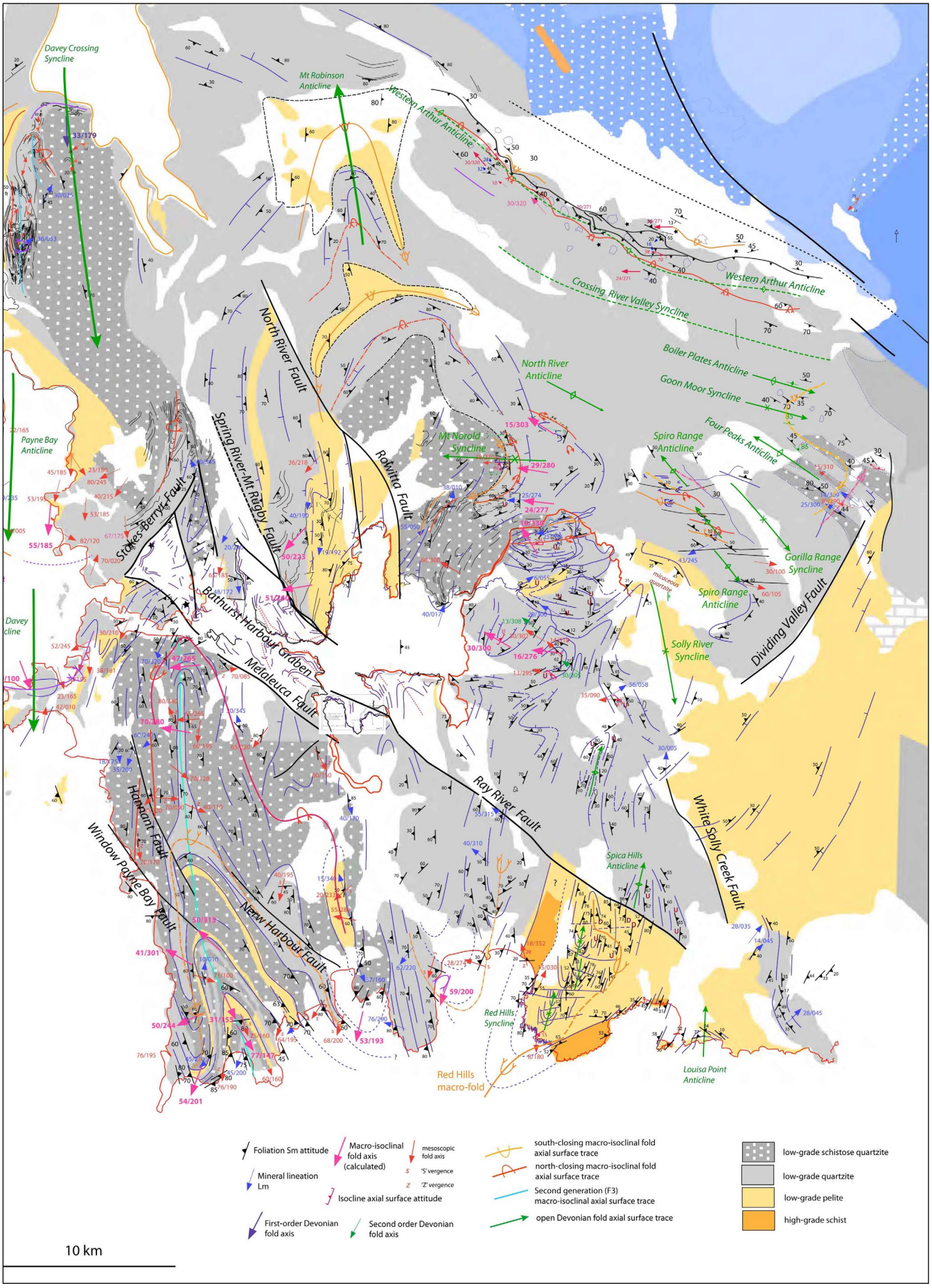

Figure 4. Structure map of the eastern part of the Southern Tyennan domain with Mineral Resources Tasmania 1:250000 digital atlas lithological base. The structural data has been compiled from mapping by Stefanski (1957a,b), Taylor (1959), BHP geologists (Hall, 1965), Williams and Lennox in 1980 (Lennox, 2013), Mulder (2013) and Mulder et al. (2015) with supplementary data from Gray and Vicary (2022a, 2022b) and Gray et al. (2022).

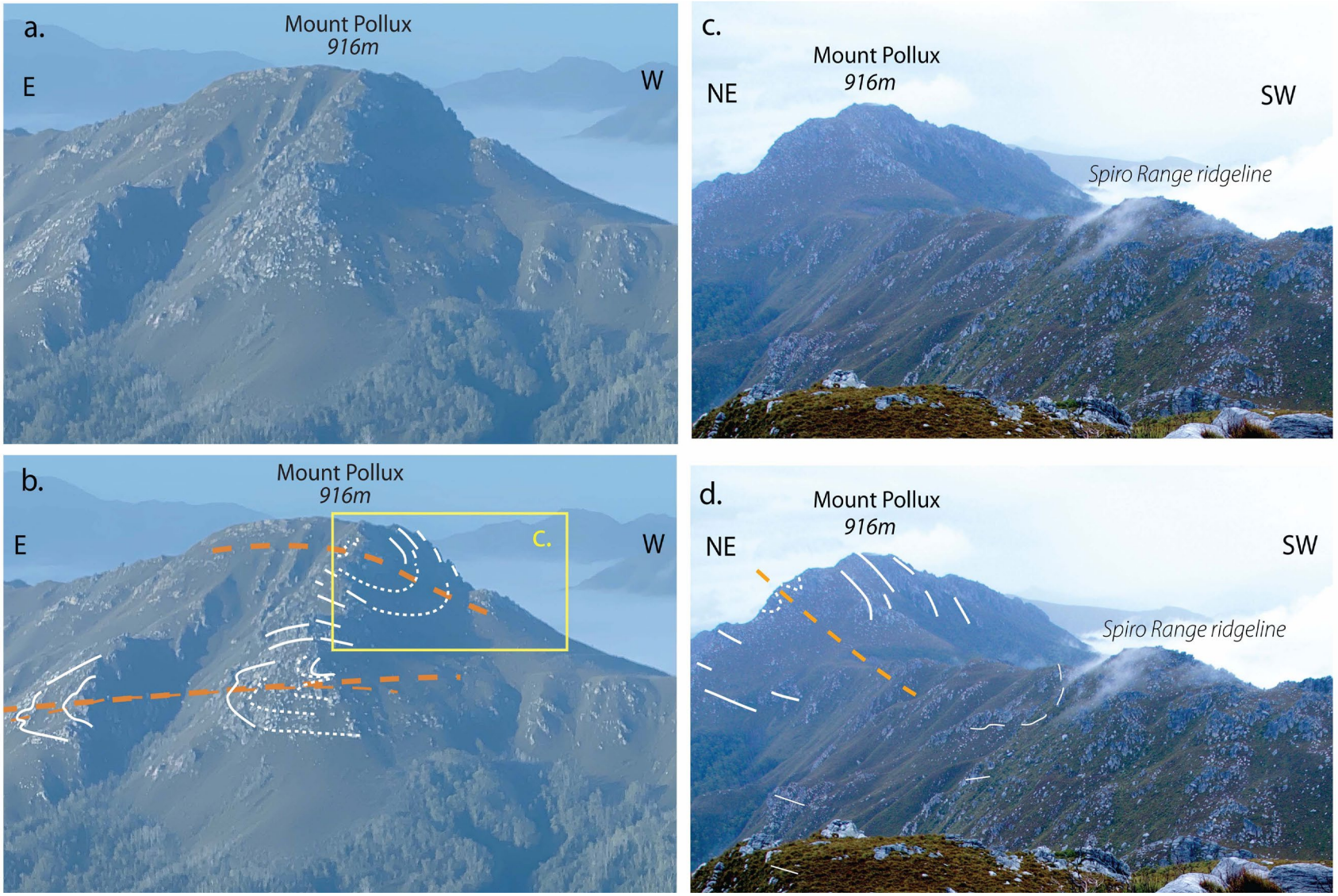

Figure 5. Helicopter and bush walker photographs of Mount Pollux (916 m) showing recumbent fold closures. These are examples of how the regional structures were interpreted across the eastern part of the Southern Tyennan domain. a) and b) annotated and non-annotated helicopter photograph of Mount Pollux looking south. The helicopter flight path was southwest along the Old River valley. An asymmetric fold pair intersects the northwest face of Mount Pollux . The southwest-closing fold hinge in shadow is structurally higher than the northeast-closing fold hinge. There is broad arching of the axial surface traces due to the younger, Devonian Spiro Range Anticline. c) and d) Annotated and non-annotated photographs of Mount Pollux looking southeast from Mount Castor. The photographs provide better definition of the structurally higher, southwest-closing macro-isocline that is in shadow in (a). Formlines in So/Sm: white and white dashed lines. Macro-fold axial surface traces: orange dashed lines. (Photo credit: Becca Lunnon, Rock Monkey Adventures)

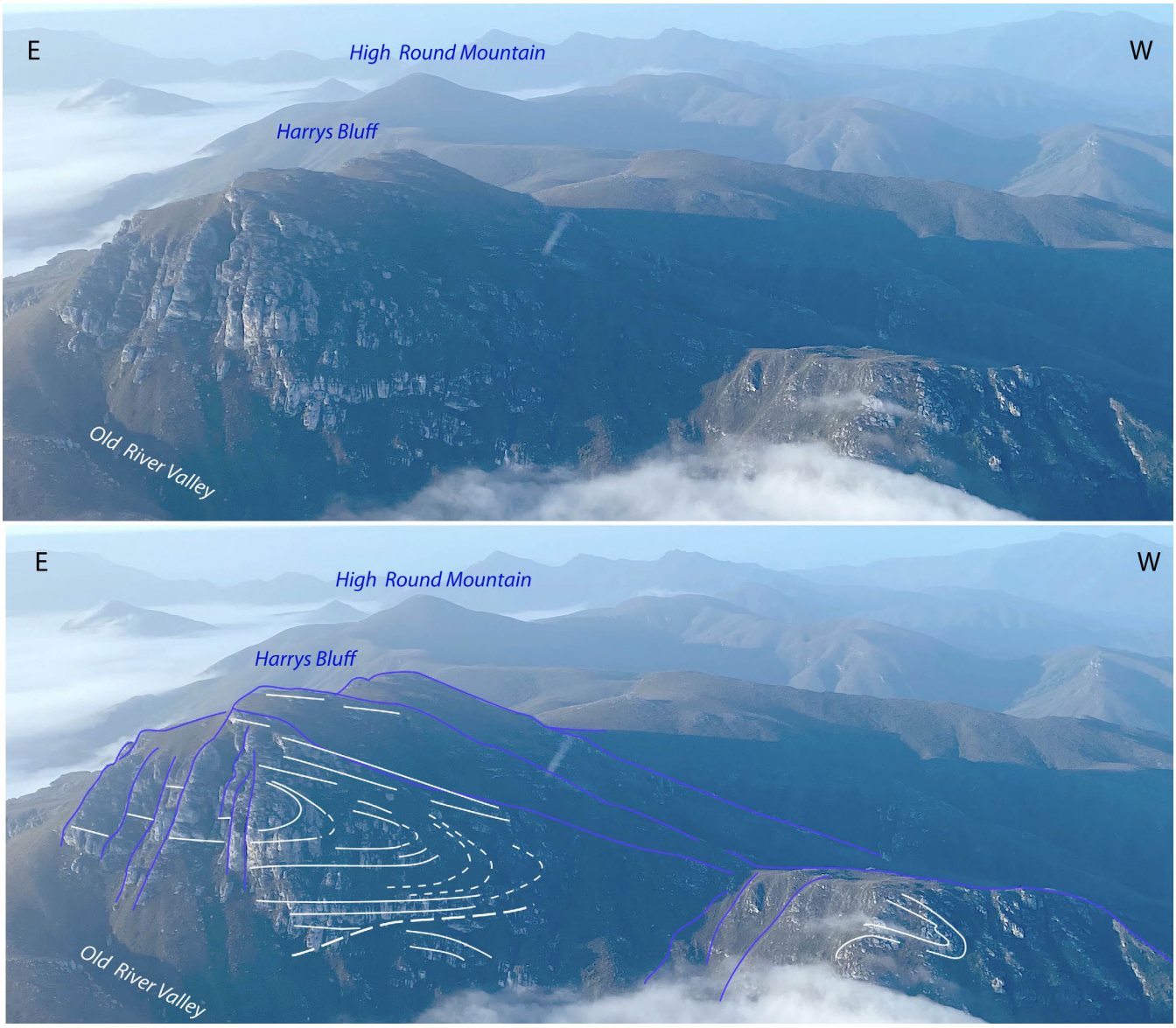

Figure 6. Helicopter photograph (a) of Harrys Bluff and High Round Mountain (background) showing an oblique view of the southwest-closing Harrys Bluff recumbent isoclinal fold. The photo is taken looking south onto the northern face of Harrys Bluff largely in shadow. The flight path was southwest along the Old River valley. b) Annotated interpretation of photograph in (a) with formlines in So/Sm (white line traces) defining the west-closing hinge. The macro-isoclinal fold plunge is 18°/330° based on mesoscopic fold data on Harrys Bluff (Figure 4). Formlines in So/Sm: white and white dashed lines.

2.0 BACKGROUND

2.1 Geographic Elements

The eastern part of the Southern Tyennan region (Figures 2 and 3) consists of hilly regions dominated by the Spiro Range, incorporating Mount Castor (773 m) and Mount Pollux (916 m), and the Ray Range, incorporating High Round Mountain (760 m), Harrys Bluff (739 m), Mount Wilson (761 m), Ripple Mountain (795 m) and Mount Norold (978 m) (Figure 3). These ranges are separated by broad, northwest-trending valleys occupied by the Old River-Collins River drainage system in the northeast and centrally by the Solly River-Watts River drainage system.

Further north the Arthur Range occupies the northeast flank of the Southern Tyennan domain (Figure 3). Made up of the northwest-trending Western Arthur Range and the more easterly north-northwest trending eastern Arthur Range it has general elevations over 1000 m. In the Western Arthur Range peaks include Mt Hayes (1119 m), Mt Sirius (1151 m), Mt Capricorn (1037 m), Mt Scorpio (1106 m) and for the Eastern Arthurs peaks include The Dial (1083 m), Federation Peak (1225 m) and Geeves Bluff (1165 m).

2.2 Map Pattern and Regional Relationships

The eastern part of the Southern Tyennan domain is clearly dominated by quartzite and schistose platy quartzite (grey areas, Figure 4), apart from in-folded, intercalations of pelite through the Rugby Range, Mt Robinson and Mt Braddon and a larger northwest-dipping pelite slab in the southeast (pale orange unit, Figure 4). High-grade schist of the Red Point Metamorphic Complex (Mulder et al., 2015) is the structurally lowest unit with two belts flanking a core of pelite within the Red Point macro-fold (bright orange unit, Figure 4).

The eastern region is split by the 20 km-long, northwest-trending, strike-slip fault-bound Bathurst Harbour graben (Figure 4). This basin contains some 2000 m of Middle Cambrian conglomerate, sandstone and mudstone of the Clytie Cove Group (Williams, 1979; Corbett & Vicary, 2015, p.174).

A major northwest-southeast trending fault on the south side of the Huon River Valley defines the northern margin of the domain and juxtaposes the low-grade Tyennan metasedimentary rocks of the Arthur Range with unmetamorphosed Proterozoic sedimentary rocks of the Clark Group and Harrisons Opening Formation to the north (blue coloured units, Figure 4).

The early, regional-scale, recumbent isoclines observed in the hillsides (Figures 5 and 6) have been refolded by younger upright, more open, east-west and north-south trending fold structures, and northwest-southeast trending folds from the Spiro Range to the Arthur Ranges. The Solly River defines a division between the northwest-southeast trending folds (Solly River Syncline and Spiro Range Anticline) and the north-south folds of the Ray Range (Figure 4).

The outcrop pattern and structural formlines in So/Sm and Sm (Figure 4) define an ovoid fold, also expressed in the topography (Figure 3), with a broad, box-like form some ~45 km in width (Figure 4). This feature is the result of fold interference between the early 2nd order macro-isoclines and the younger Devonian north-south trending, east-west trending and northwest-trending open folds (Figure 4).

The quartzite structure appears as a series of recumbent folds or a recumbent, isoclinal macro-fold pair, as previously delineated in the Eastern Arthur Range (Gray & Vicary, 2022a). The fold pair can be seen in the Spiro Range and the structurally highest parts of the Mt Norold-Harrys Bluff-High Round Mountain quartzite domain (Figures 5 and 6) with axial trace length scales >20 km. South of Harrys Bluff the quartzite shows fold interference between east-west and north-south trending folds (Figure 4), as well as truncation by late Cambrian basin-controlling, oblique- slip normal faults (Figure 4).

2.3 Lithology and Litho-Tectonic Units

Several authors (Stefanski, 1957a, b; Taylor, 1959; Lennox, 2013) have established a litho-stratigraphy, with the initial subdivision by Stefanski (1957a) into an older and younger Precambrian quartzite-pelite series, with the following stacking in the Older Series from top to base:

quartzite (Q, MQ) > (overlying) schistose quartzite+quartz mica schist+mica schist (QSS, AQ) > phyllite (A), with Q: quartzite, MQ: massive quartzite, QSS: quartzite and quartzitic sandstones withcross-bedding and ripple marks, AQ: interlayered quartz-mica schists, phyllite and thin quartzite bands.

The subdivision by Lennox (2013) was massive quartzite, micaceous quartzite and phyllite units, with the Harrys Bluff cliff exposure showing quartzite, overlying a thin zone of micaceous quartzite, overlying low-grade pelite (phyllite).

Quartzite with a 650-700 m apparent thickness occupies the ridges with schist/phyllite in the valleys (see Taylor, 1959, Figure 9).

2.4 Nature of the Layering

The dominant foliation/layering in quartzite and pelite sequences is a bedding-parallel foliation (So/Sm) or transposition layering Sm (Figure 7). Cross-bedding (Figure 8) and ripple marks on bedding surfaces are preserved in places, particularly in the Harrys Bluff, High Round Mountain and Red Hills areas (Lennox, 2013). In places it is a differentiated metamorphic layering with complex origin (Figures 9 and 10), suggesting the deformation is very heterogeneous (Lennox, 2013).

The low-grade phyllite also shows a millimetre-scale differentiated layering character (Figure 10). The phyllite displays transposition layering as a millimetre -spaced foliation typified by segmented, discontinuous, quartz -rich lenticle-like fragments in a micaceous matrix, where the mica fabric of the rock matrix is sub-parallel to the spaced foliation.

2.5 Basal High Strain Zone

Structural mapping near Harrys Bluff and Mt Pollux, Spiro Range by Williams and Lennox respectively in 1980 (Lennox, 2013) suggests the structurally lowest part of the quartzite unit is transitional into a basal zone of intense foliation Sm characterised by schistose and platy quartzite, with refolding of early isoclines and overprinting multiple fabrics (Figures 7 and 11).

A thin section of sample BA7 (Figure 11, from Lennox, 2013, Plate 2) from the lower slopes of the Spiro Range towards the base of the quartzite and the contact with the underlying low-grade pelite shows lenticular, rootless quartz-rich layers (So/Sm) in-folded with mica-rich layers (So/Sm) by mesoscopic to microscopic isoclinal folding (Figure 11). The now rootless folds commonly have an axial surface primary mica S1 cleavage fabric (slaty-type) that is folded by an early crenulation cleavage fabric (Scc1) at low angles to So and S1 (Figure 11b). These are sub-parallel with a pronounced compositional banding (So/Sm) and a developing dominant foliation Sm (heavy pink traces, Figure 11b). In outcrop the dominant foliation would appear as pronounced, transposed compositional banding sub-parallel to or at very low angles to the complex early fabrics. In this sample a younger crenulation cleavage Scc2 crenulates So/Sm, S1, and Scc1 (Figure 11b).

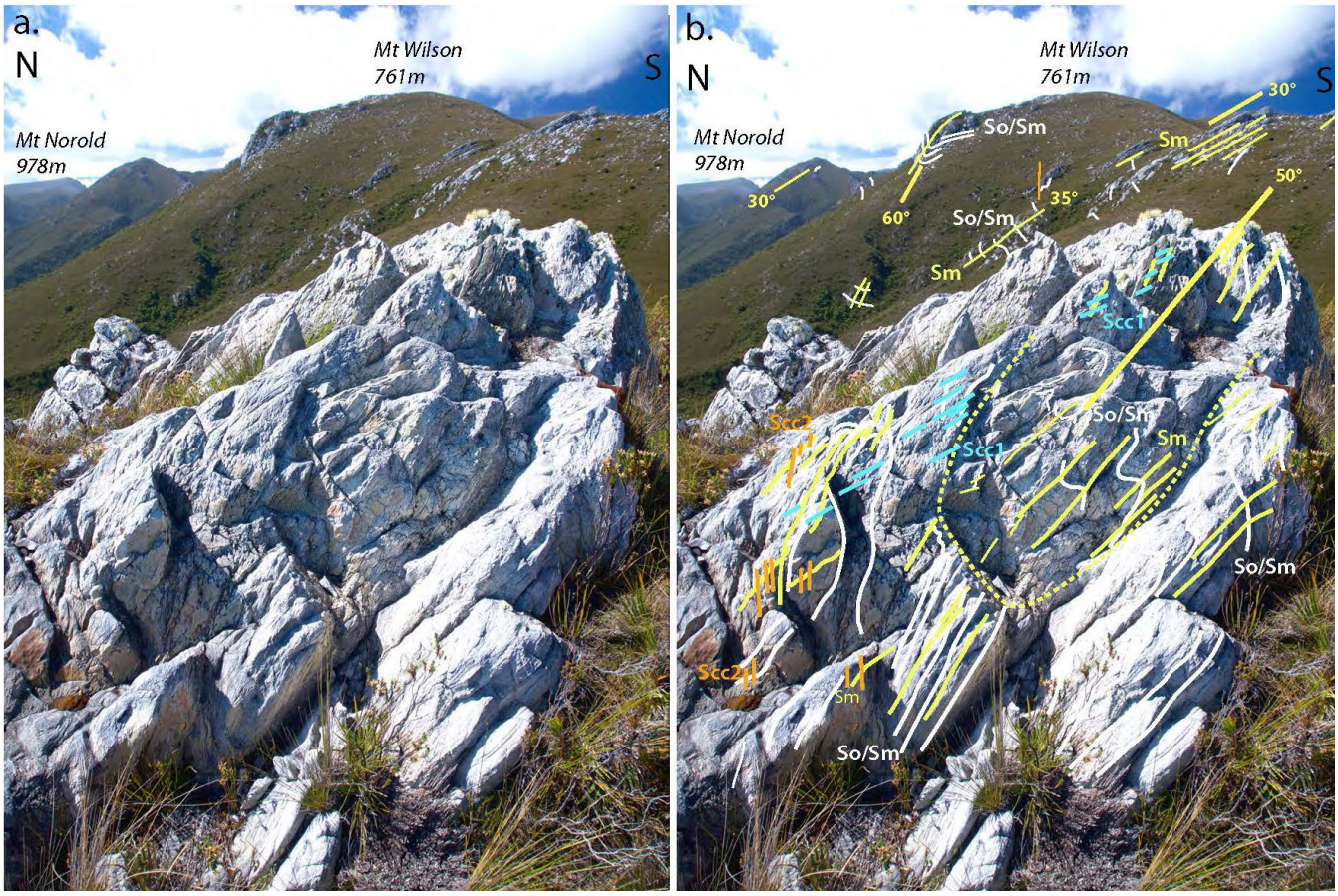

Figure 7. Intensely deformed quartzite outcrop on the southwest ridgeline flank below Mt Wilson. a) and b) are non-annotated and annotated photographs respectively. White line traces: So/Sm; Yellow line traces: Sm; Blue line traces: Scc1; Orange line traces: Scc2. Generalised Sm in the quartzite outcrop is dipping at 50° NW. A northwest closing recumbent isoclinal fold hinge is visible in the northwest flank of Mt Wilson with this outcrop part of a high-strain zone developing along the recumbent fold lower limb. This appears arched by a younger upright, east-west trending anticline through Mt Wilson with Scc2 as axial surface cleavage (orange traces).

(Photo Credit: Becca Lunnon, RockMonkeyAdventures)

Figure 8 (left). Cross-bedding in quartzite on Harrys Bluff with view to the east showing Federation Peak and Mount Geeves on the back ridge, with Mount Pollux on the Spiro Range (photo to right in the middle ground). a) and b) are non-annotated and annotated photographs respectively. b) Formline interpretation showing So/Sm traces (white lines) and younger cleavaged (green traces). The outcrop on Harrys Bluff (photo left) indicates the quartzite is right way up. (Photo credit: Becca Lunnon, RockMonkeyAdventures)

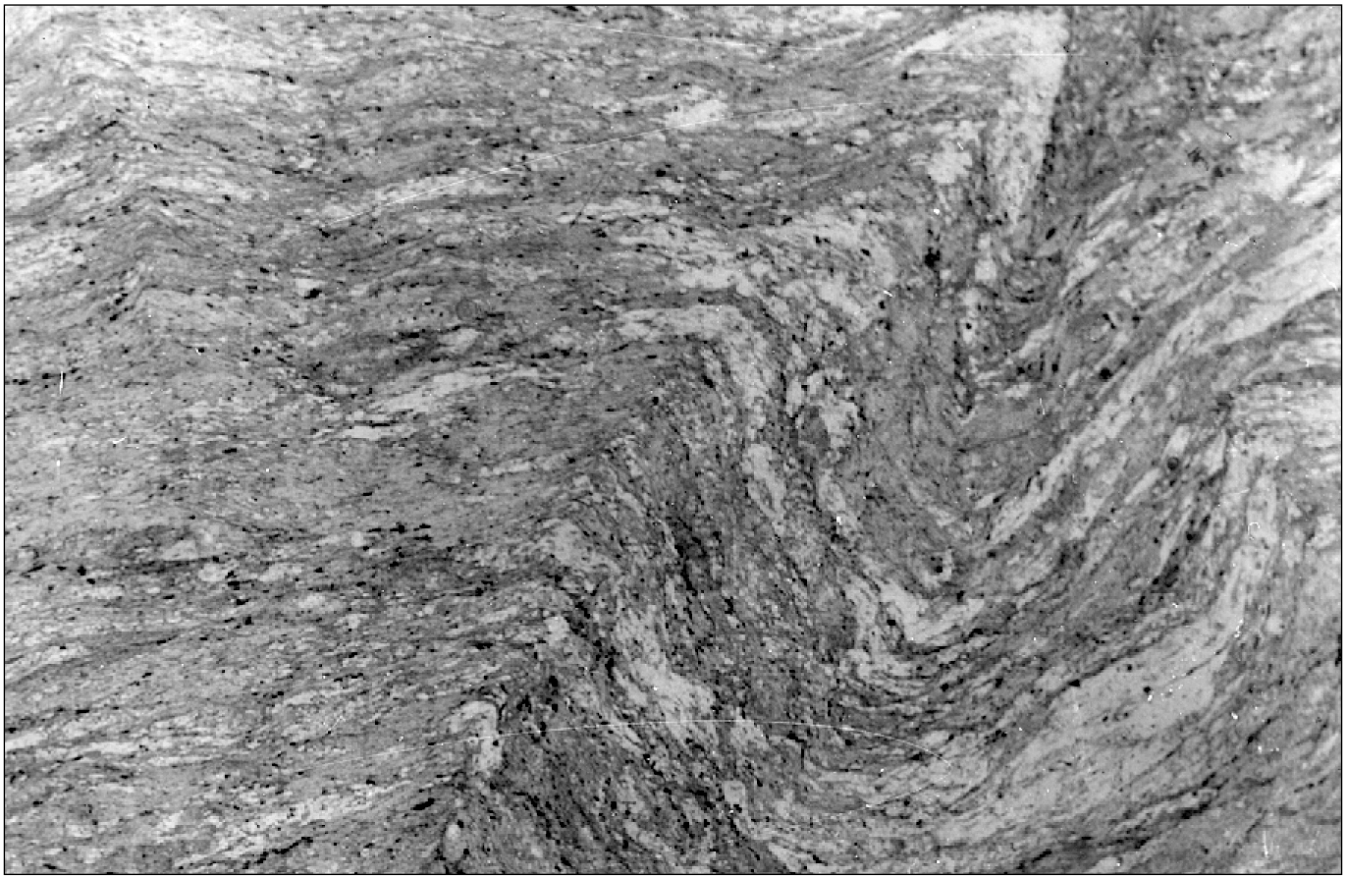

Figure 9. Photomicrograph of differentiated metamorphic layering in meta-quartzite, Spica Hills (Lennox, 2013, Plate 6). The spacing between quartz-rich and mica-rich zones varies between1.5 mm and 2 mm. Sample BA13, Spica Hills (448800/5185300).

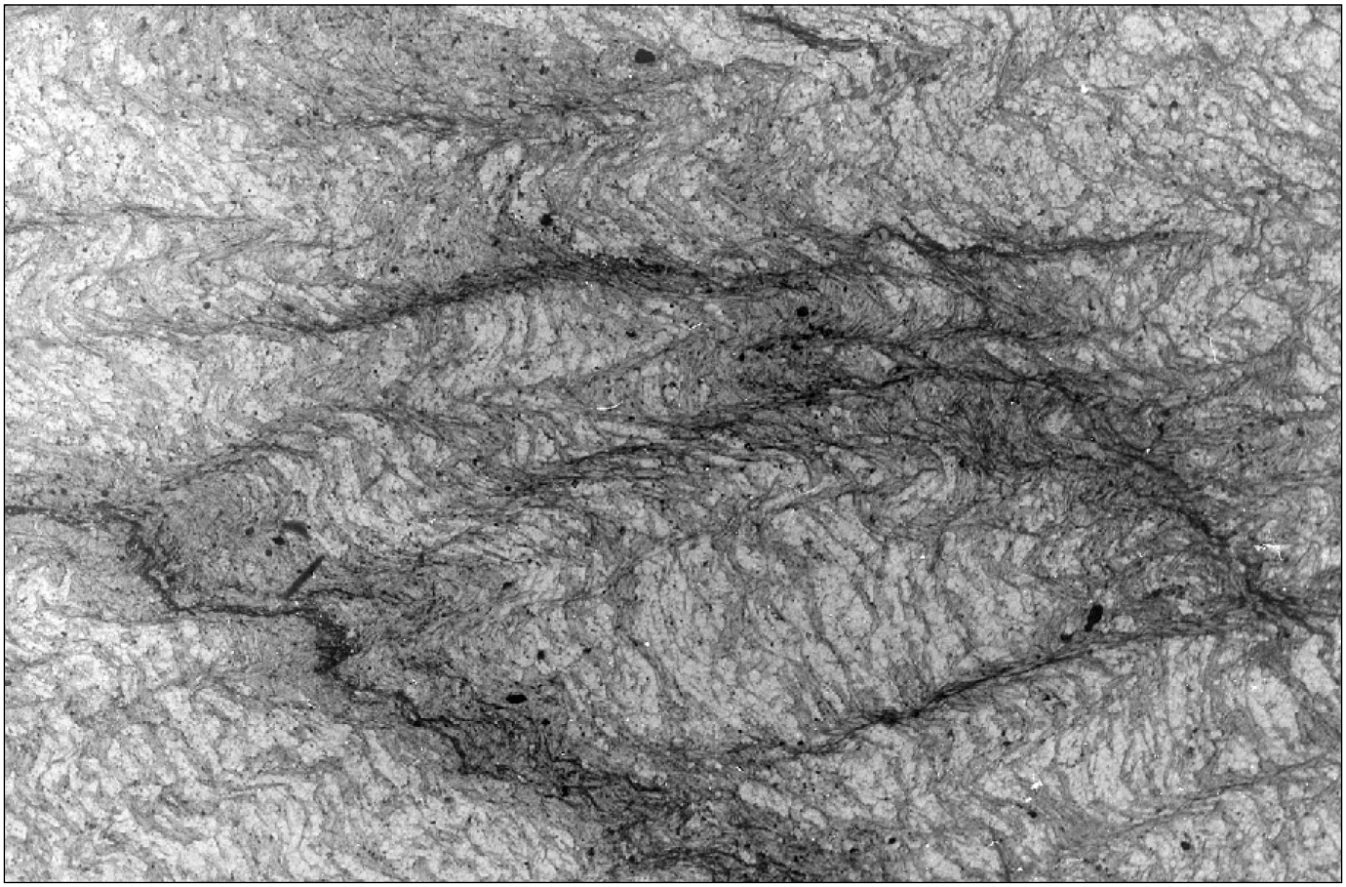

Figure 10: Photomicrograph of segregated metamorphic layering in phyllite, eastern end of Ray Range (Lennox, 2013, Plate 3). Sample BA6 (445500/5195300).

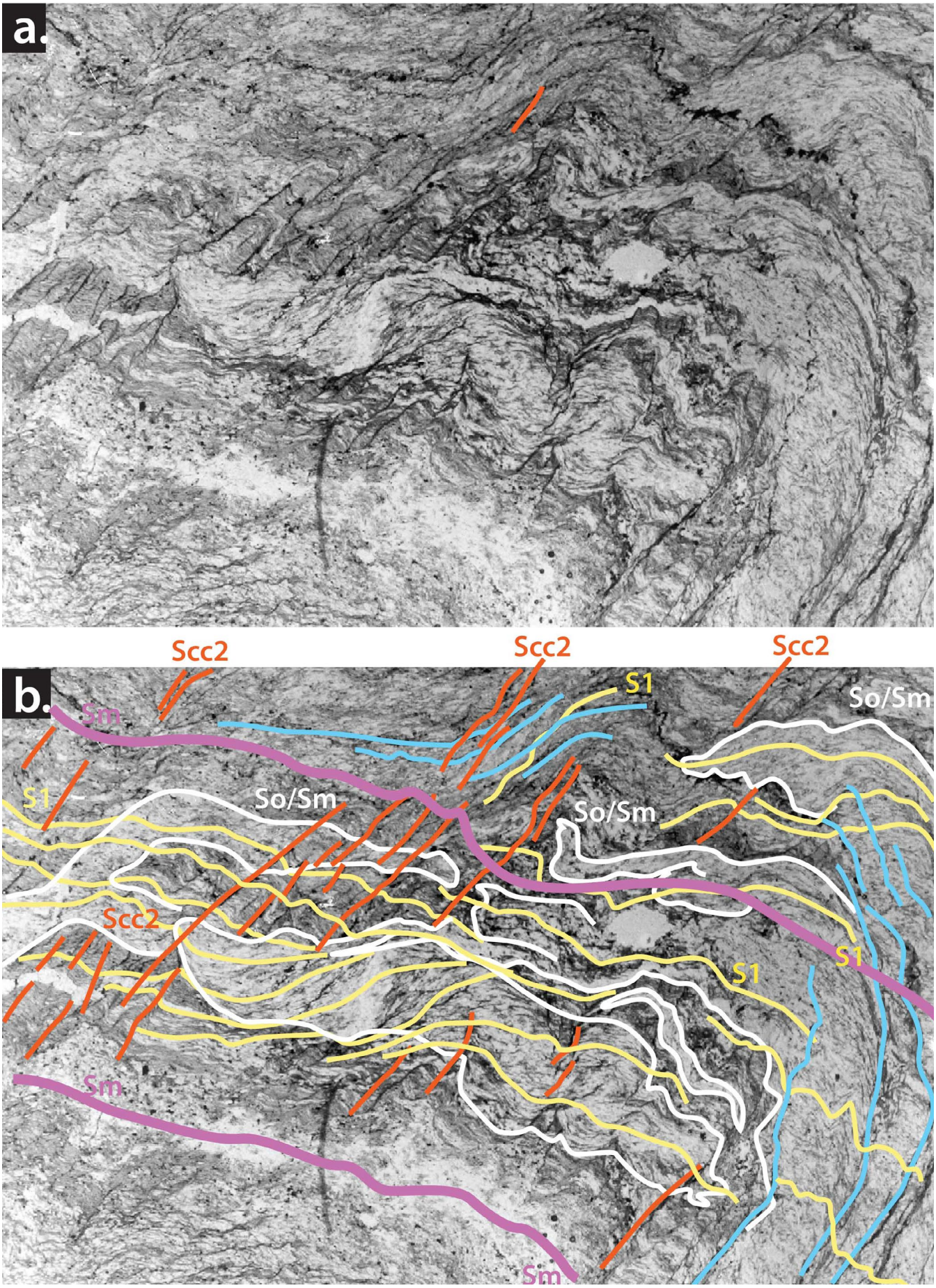

Figure 11. Photomicrograph of complexly deformed micaceous quartzite in basal high strain zone to the quartzite, lower slopes of Mt Pollux, Spiro Range (Lennox, 2013, plate 2). Sample BA7 (449000/5203700).

So/Sm: compositional banding (white line traces). S1: primary slaty cleavage axial surface to relict isoclines in So/Sm (yellow line traces). Scc1: first crenulation cleavage folding S1 and at low angles to S1 (blue line traces). Scc2: second crenulation cleavage that folds all the earlier-formed fabrics (orange line traces). Sm: dominant foliation (heavy purple line traces).

2.6 Current Structural Compilation

The structural interpretation and discussion is based on interpretation of 1) oblique aerial photographs of hillsides taken during the helicopter visits, 2) bushwalker photographs of peaks and ridgelines, linked with 3) ListMap air photo interpretation, and constrained by 4) limited outcrop measurements and observations. The structural data presented has been generated from mapping by Stefanski (1957a, b), Taylor (1959), BHP geologists (Hall, 1965), Williams and Lennox in 1980 (Lennox, 2013), Mulder (2013) and Mulder et al. (2015).

The hillside and cliff photograph interpretations in combination with limited structural data enabled structural profile construction that provided the basis for the regional structural interpretation. It is important to note that nofield checking and/or structural data collection has been undertaken by the authors in this part of the Southern Tyennan domain.

All map grids and grid references in the text have a GDA94 datum with MGA coordinates in Zone 55.

The following **structural terminology** is used:

So/Sm	metamorphic foliation parallel to bedding (commonly a transposition layering)
So/Sm env	enveloping surface to folded So/Sm
Sm	dominant or main metamorphic foliation
Sb	shear band (S-C' structure)
AST	fold axial surface trace
AS/Sm	dominant foliation sub-parallel to fold axial surfaces
Sm/Sb	dominant foliation developing from Sb, shear band foliation
Scc	crenulation cleavage
Scl	Devonian overprinting low-grade cleavage
S1	early slaty cleavage
Lm	dominant lineation
Lstretch	stretching lineation
Lelongation	mineral elongation lineation
TD	transport direction
Lint	intersection lineation
Lrod	rodding lineation developed from deforming Lint
FA	fold axis
F1, F2, F3	local age of fold axes (oldest to youngest)
Lm^FA	angle between Lm and FA
Sm^Sb	angle between Sm and Sb

3.0 EASTERN SOUTHERN TYENNAN STRUCTURAL GEOLOGY OVERVIEW

The eastern part of the Southern Tyennan domain consists of three wavelength-based orders of early, major isoclinal fold structures (Figure 12). These are:

- 1st order regional isoclinal fold-nappe with an axial surface trace length of ~30 km extending from Mt Braddon southwards through the Rugby Range to the Bathurst graben and a nappe core thickness of ~15 km in profile incorporating the pelite and quartzite layers. The fold-nappe represents the attenuated northern closure of the South West Cape mega-sheath fold system (Gray and Vicary, 2022b).
- 2nd order regional-scale isoclinal folds with wavelengths of ~5 km. These are map-scale folds involving folding of both pelite and quartzite units, where the pelite is infolded with the quartzite (Figure 12). The map outcrop patterns at Mt Robinson and Mt Braddon (Figure 4) show the pelite isolated in the quartzite due to mushroom or Type 2 fold interference (Ramsay, 1967).
- 3rd order isoclinal macro-folds with wavelengths of 400-450 m. These are exposed in cliffs and hillsides preserved mainly within the quartzite litho-tectonic layer or unit (Figures 5 and 6).

3.1 1st Order Regional Fold nappe

The northern close-out or lateral termination of the South West Cape mega-sheath fold (Figure 13) has a refolded plunging fold-nappe geometry (Figure 14b and d). Refolding by the north-south trending younger Devonian folds has caused a swing from north-trending along the Rugby Range to east-trending through Mt Robinson and Mt Braddon to produce the type 2 fold interference pattern (Figure 13).

A north-south cross section along the Mt Robinson Anticline hinge (Figure 14b and c) shows the major fold-nappe hinge has "la tete plongee" geometry or "diving fold nose". The second-order folds are symmetrical with 'W' symmetry and define the larger, downward-closing nappe hinge (Figure 14). Platy quartzite occurs on the upper limb (Davey Saddle area) and on the lower limb (North River Valley and Rowitta Plains) (Figure 14a and b). The fold-nappe is cored by low-grade pelite that "rolls" from sub-vertical to sub-horizontal in the plane of the cross section as So/Sm changes to a north-south strike with a west dip through the Rugby Range. The fold-nappe axial surface trace is truncated and offset by two, northwest-trending, sub-vertical, dextral oblique-slip faults related to the mid-Cambrian Port Davey-Bathurst Harbour graben development (Figures 13 and 14a).

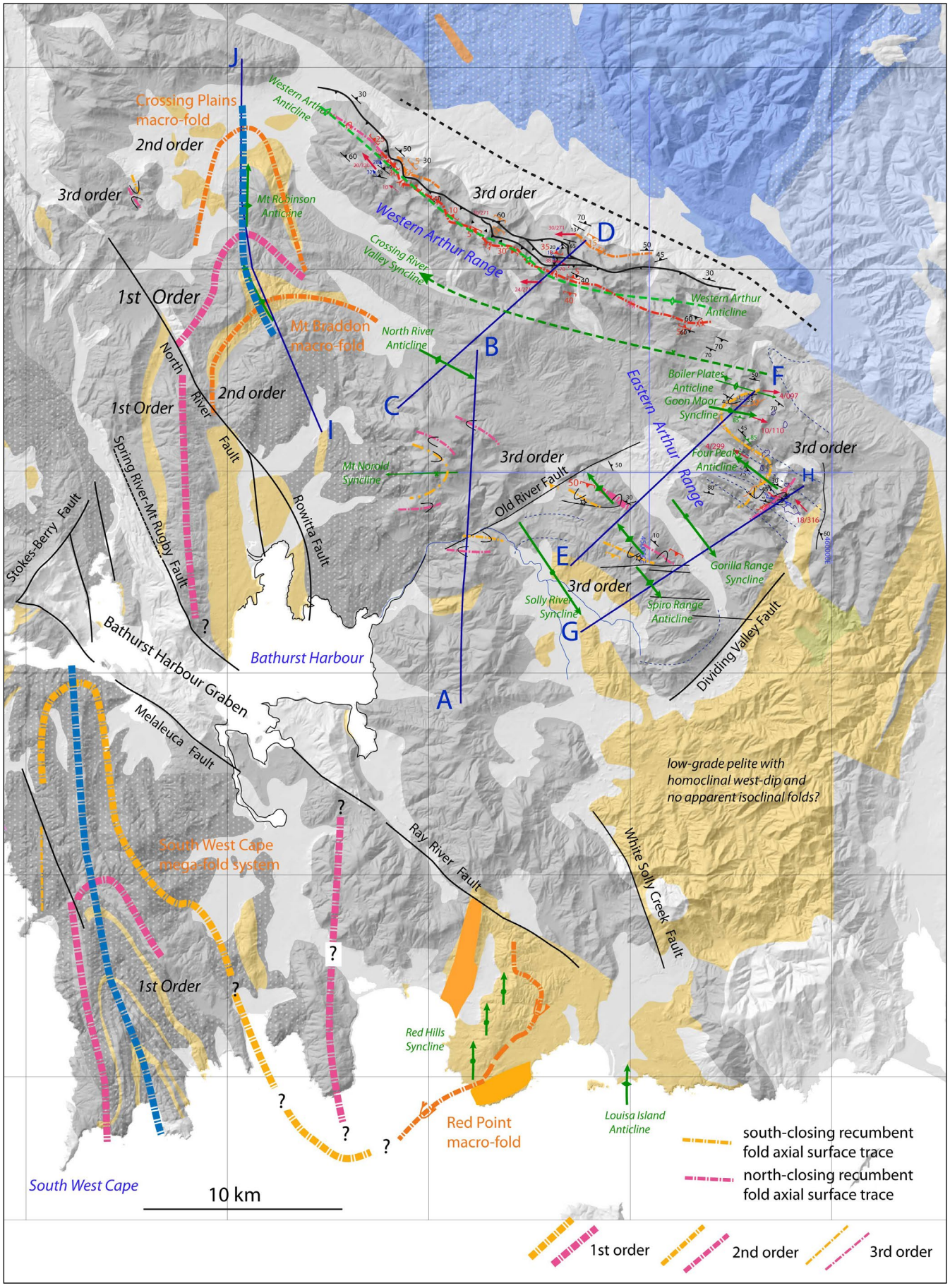

Figure 12. Fold axial surface trace (AST) map showing south-closing (orange dashed line trace) and north-closing (pink dashed line trace) isoclinal axial surface traces of the early macro-folds. Fold order is differentiated by the axial surface (AST) line thickness. The heavy blue dashed line represents the axial surface traces of second generation isoclinal macro-folds that refold the early-formed macro-folds within the core of the South West Cape mega-sheath fold. Younger Devonian fold traces are shown by the green line traces. Faults are shown by black line traces. Section lines A-B, C-D, E-F, G-H and I-J are shown by the dark blue lines. Map base is the Mineral Resources Tasmania 1:250000 digital atlas draped over DEM. For the Mt Robinson and Mt Braddon areas the main axial surface trace AST (pink dashed line) lies within quartzite (grey) and splits the pelite (orange) bands.

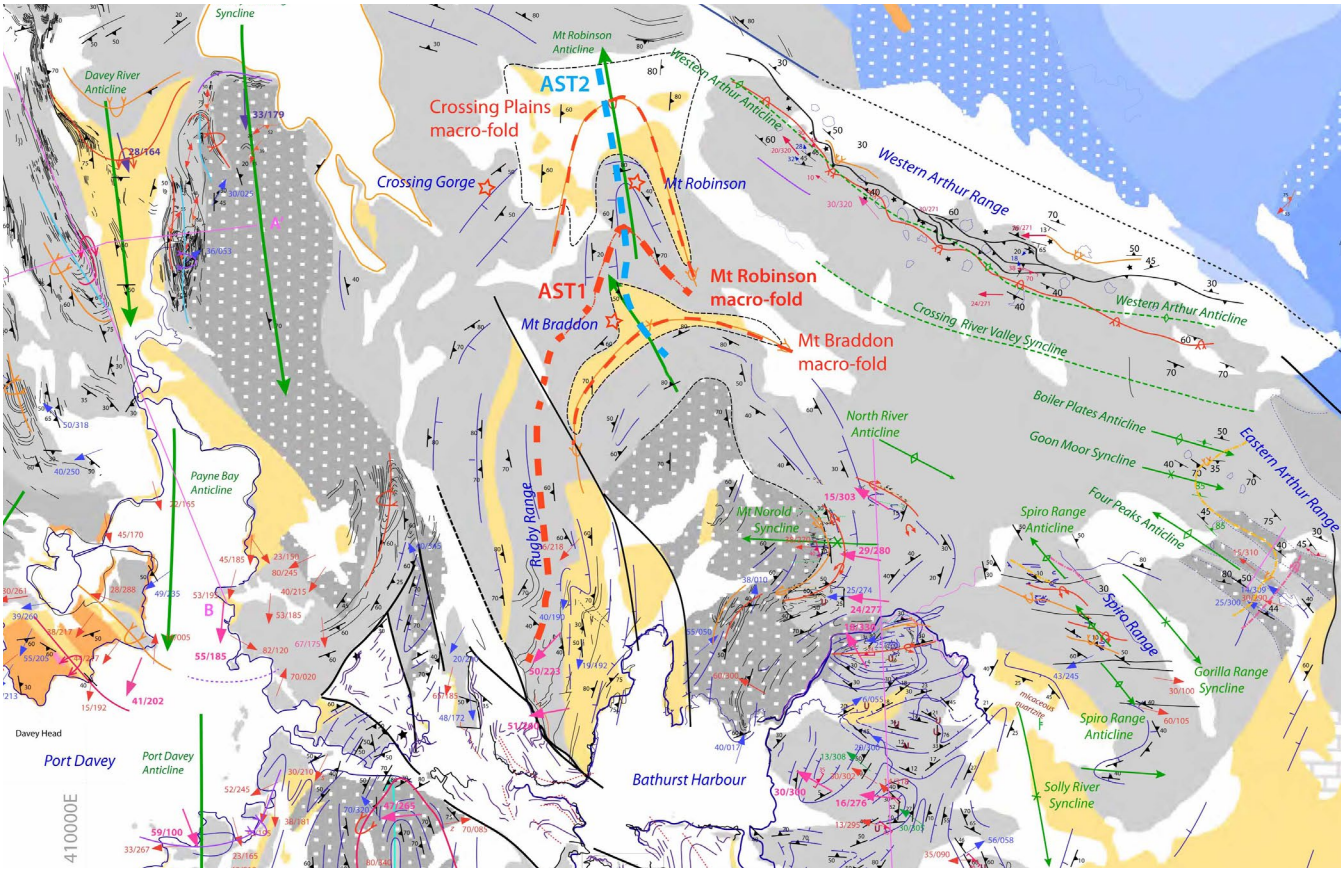

Figure 13: Structure map of the northern termination of the South West Cape mega-sheath fold system showing the Type 2 fold interference patterns of infolded pelite within the Crossing Plains (molar-tooth shape) and Mt Braddon (sombrero shape) hinges. The main axial surface trace is shown by the pink dashed line. The base map is from the Mineral Resources 1:250000 digital atlas. Red dashed lines: Early Fold F1 macro-fold axial surface traces. Blue dashed line: second phase F2 macro-isocline fold axial surface trace. Green line traces: Devonian fold axial surface traces. Faults: thin black lines.

A north-south cross section along the Mt Robinson Anticline hinge (Figure 14b and c) shows the major fold-nappe hinge has "la tete plongee" geometry or "diving fold nose". The second-order folds are symmetrical with 'W' symmetry and define the larger, downward-closing nappe hinge (Figure 14). Platy quartzite occurs on the upper limb (Davey Saddle area) and on the lower limb (North River Valley and Rowitta Plains) (Figure 14a and b). The fold-nappe is cored by low-grade pelite that "rolls" from sub-vertical to sub-horizontal in the plane of the cross section as So/Sm changes to a north-south strike with a west dip through the Rugby Range. The fold-nappe axial surface trace is truncated and offset by two, northwest-trending, sub-vertical, dextral oblique-slip faults related to the mid-Cambrian Port Davey-Bathurst Harbour graben development (Figures 13 and 14a).

3.2 2nd Order Regional Isoclinal Folds

3.2.1 Crossing Plains and Mt Braddon Isoclinal Macro-folds

These folds are defined by pelite infolded with quartzite in a Type 2 mushroom fold interference pattern (Figures 12 and 13). The early isoclinal hinges are refolded by a north-south trending, tight to isoclinal antiformal fold (Mt Robinson Anticline). β determinations for the Mt Braddon macro-fold hinge in pelite give 42°/250° (west closure), 13°/052° (middle part of closure) and 54°/270° (east closure) with an axial surface fit of 235°/71°NW. β determination for a hinge in the platy quartzite gave 58°/264° (Figures 14a and 15e).

The Mt Robinson Anticline (Figure 15) has complex character with steep to sub-vertical limbs and hinge, and almost isoclinal form in places along the hingeline (Figure 13). Fold plunge is typically steep with hinge segments dipping at 80° north or south (Figure 15a). The tight to isoclinal nature of the Mt Robinson Anticline suggests that this is 1) not a simple, open Devonian anticline, and 2) more likely a Devonian coplanar fold-tightening of an early-formed Cambrian second generation isoclinal macro-fold. As such this second-generation isoclinal macro-fold refolds the first-generation F1/F2 Crossing Plains and Mt Braddon isoclinal macro-folds, as well as the major fold-nappe hinge that they are part of (Figures 12 and 14a, b). Second generation isoclinal macro-folds are shown by the dashed blue axial surface line traces (AST) in Figures 12, 14a and 14d.

Similar geometrical relationships occur within the inner shell and Davey River nose of the De Witt-Propsting mega-sheath fold and the core of the South West Cape mega-sheath fold (see Gray and Vicary, 2022b) where approximately upright, second-generation isoclinal macro-folds refold early-formed, first-generation isoclinal macro-folds (Gray and Vicary, 2022b).

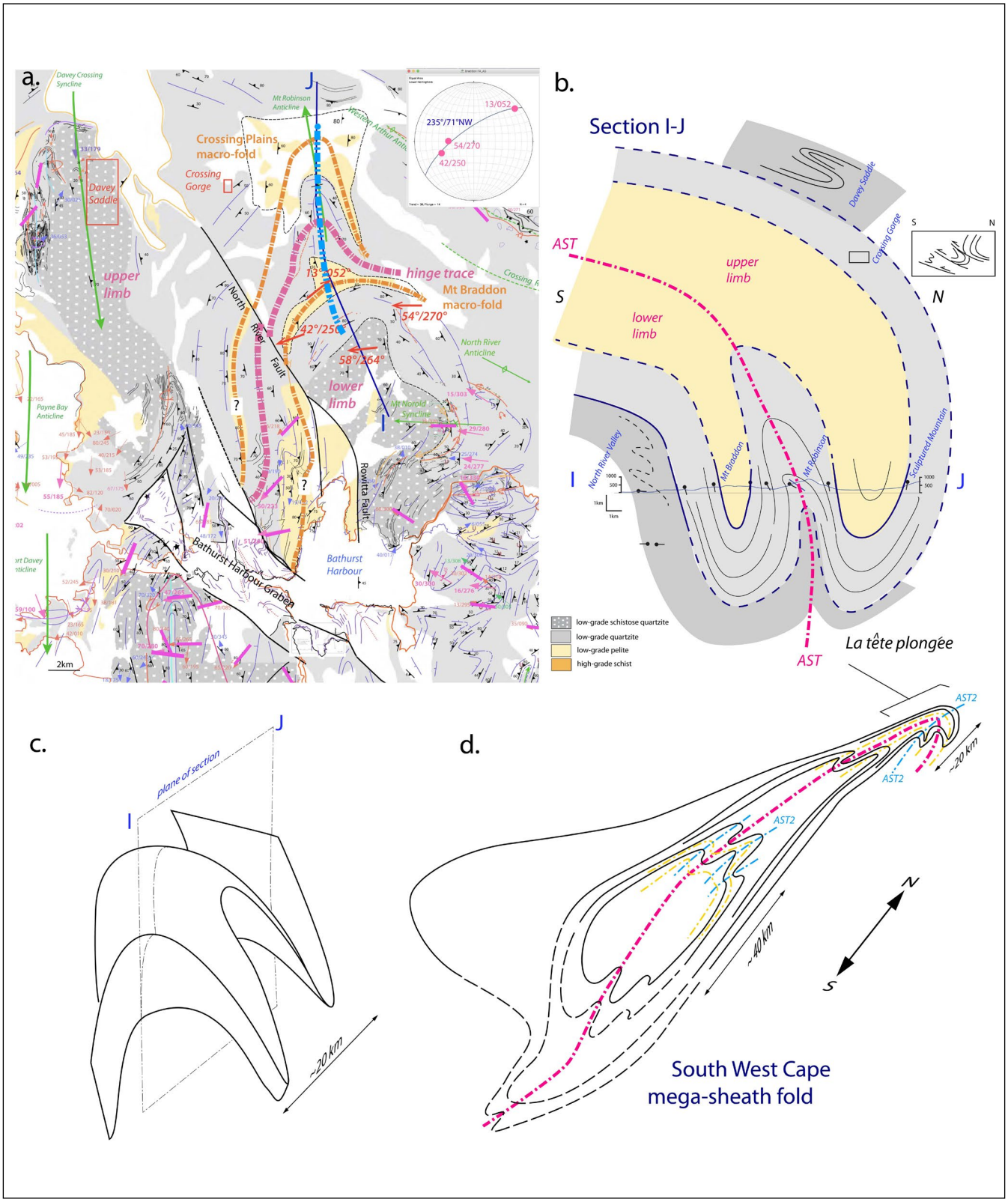

Figure 14. 2nd order folds and the northern termination of the South West Cape mega-sheath fold. a) Axial surface trace map of the northern sheath-fold termination incorporating the Crossing Plains and Mt Braddon macro-fold hinges (orange dashed axial surface traces). The main axial surface trace is shown by the pink dashed line. The base map is from the Mineral Resources 1:250000 digital atlas. The red arrows show calculated (β determination) fold plunges for parts of the Braddon macro-fold. Inset stereonet shows best-fit great circle (235°/71°NW) to the calculated fold axes. The location of the section line I-J is shown (blue line trace). b) Section I-J along the hingeline of the Mt Robinson anticline. The profile extends from the Rowitta Plains to Sculptured Mountain. c) 3D schematic diagram illustrating the geometry of the Type 2 fold interference at Mt Robinson and Mt Braddon. d) Schematic 3D interpretation of the west-closing South West Cape mega-sheath fold. The sectional view is an oblique map projection used to construct the sheath form aided by mesoscopic fold axis plunges. The northern prolongation of the sheath-fold represents the attenuated and refolded fold-nappe geometry shown in (b). First phase isoclinal fold axial surface traces are shown as pink and orange dashed lines. Second phase isoclinal fold axial surface traces are shown by the blue dashed lines (AST2).

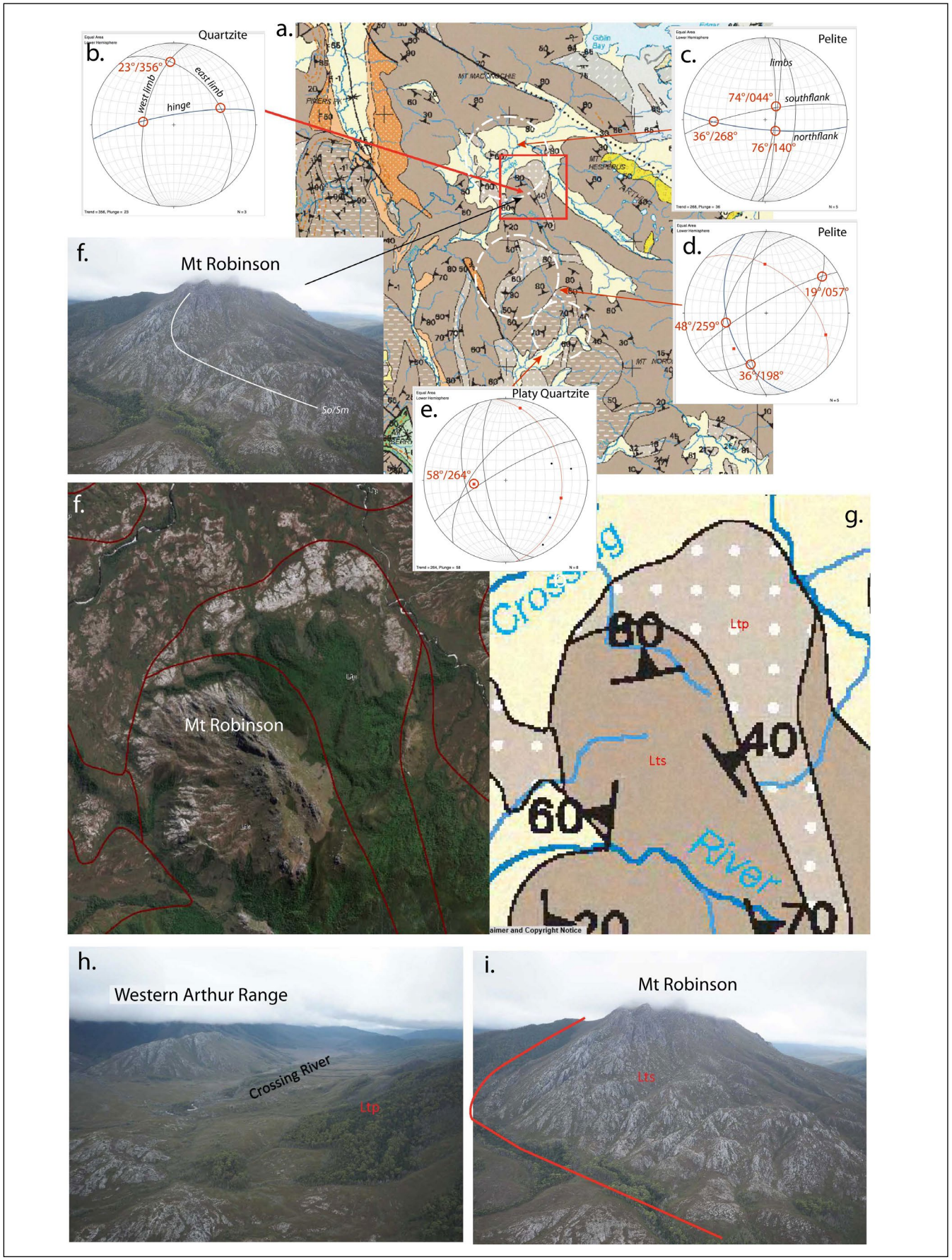

Figure 15: Photographs maps and fold plunge data as stereonets for the complex refolded Mt Robinson and Mt Braddon region. a) Mt Robinson-Mt Braddon region of the Mineral Resouces Tasmania 1:250000 geological atlas showing the positions of photographs and the structural data plotted in stereonets. b) Stereonet of the So/Sm attitude data defining the hinge of the Mt Robinson Anticline in quartzite. β intersection fold axis plunges are shown by the red circles and red text. c) Stereonet of the So/Sm data in the Crossing Plains macro-fold hinge in pelite. d) Stereonet of the So/Sm data in the Mt Braddon macro-fold hinge in pelite. β intersection fold axis plunges are shown by the red circles and red text. e) Stereonet of the So/Sm data in platy quartzite of the data of the Rowitta Plains. β intersection fold axis plunges are shown by the red circles and red text. f) Google satellite image of Mt Robinson. g) Geological map of Mt Robinson from the Mineral Resources Tasmania 1:250000 geological atlas. h) View to the northeast of the pelite exposures in the Crossing Plains macro-fold hinge. i) Aerial photograph of Mt Robinson within quartzite.

3.2.2 Red Point Isoclinal Macro-fold

The Red Point Isoclinal macro-fold (element 7, Figure 1) is another 2nd order macro-fold that occupies the lower structural levels of the Southern Tyennan domain. It is interpreted as a south-closing fold within high-grade schist cored by low-grade pelite, where the hinge is not preserved but lies offshore in Cox Bight (Figure 16). The structurally higher western limb is the northern schist belt (the NMGS of Mulder et al., 2015) along the Black Cliff Hills with a generalised attitude of 200°/45°W. The structurally lower southern limb is the southern schist belt (the SMGS of Mulder et al., 2015) with a generalised attitude of 240°/65°W. The inferred early macro-fold has an approximate reclined geometry with a plunge of 43°/270°.

Younging data from Lennox (2013) and Mulder (2013) suggest the western, structurally higher limb (the NMGS) is structurally overturned but with right-way-up younging, whereas the southeastern structurally lower limb (the SMGS) has upside-down younging (Figures 16 and 17a). The axial surface trace (AST) of the macro-fold separates domains of right-way-up younging on the upper limb from upside younging beds on the lower limb (Figure 16).

The macro-fold hinge is offset by a series of east-west trending, sub-vertical dextral faults (Figure 16) and the southern part of the hinge is thinned by the high strain zone through Contact Cove (Mulder et al., 2015; Gray and Vicary, 2022c). This structure has been refolded by the north-south-trending open folds that dominate the Red Point Hills (Figure 17b). Both fold sets have been offset by east-west-trending brittle faults and reactivated high-strain zones (Figure 16).

3.3 3rd Order Regional Isoclinal Folds

3.3.1 Geometry of 3rd Order Folds

The apparent widespread distribution of these 3rd order isoclinal macro-fold hinges (Figure 12), suggest that this part of the Southern Tyennan domain consists of a stack of recumbent isoclinal folds largely preserved in the quartzite sequence. The folds however consist of an S-vergent, asymmetric fold pair that has been folded and reoriented by the younger Devonian fold sets (green fold axial traces, Figure 18).

These younger Devonian folds are west-northwest trending in the Western Arthur Range swinging to northwest trending from the Eastern Arthur to the Spiro Range, to east-west trending in the central part from Mt Norold through Harrys Bluff and High Round Mountain to Maatsuyker Island, with minor north-south trending folds occur in the Red Hills-Louisa Point area (Figures 12 and 18) but becoming more prominent in the northwest as shown by the Davey Crossing Syncline and the reactivated Mt Robinson Anticline (Figures 14 and 15).

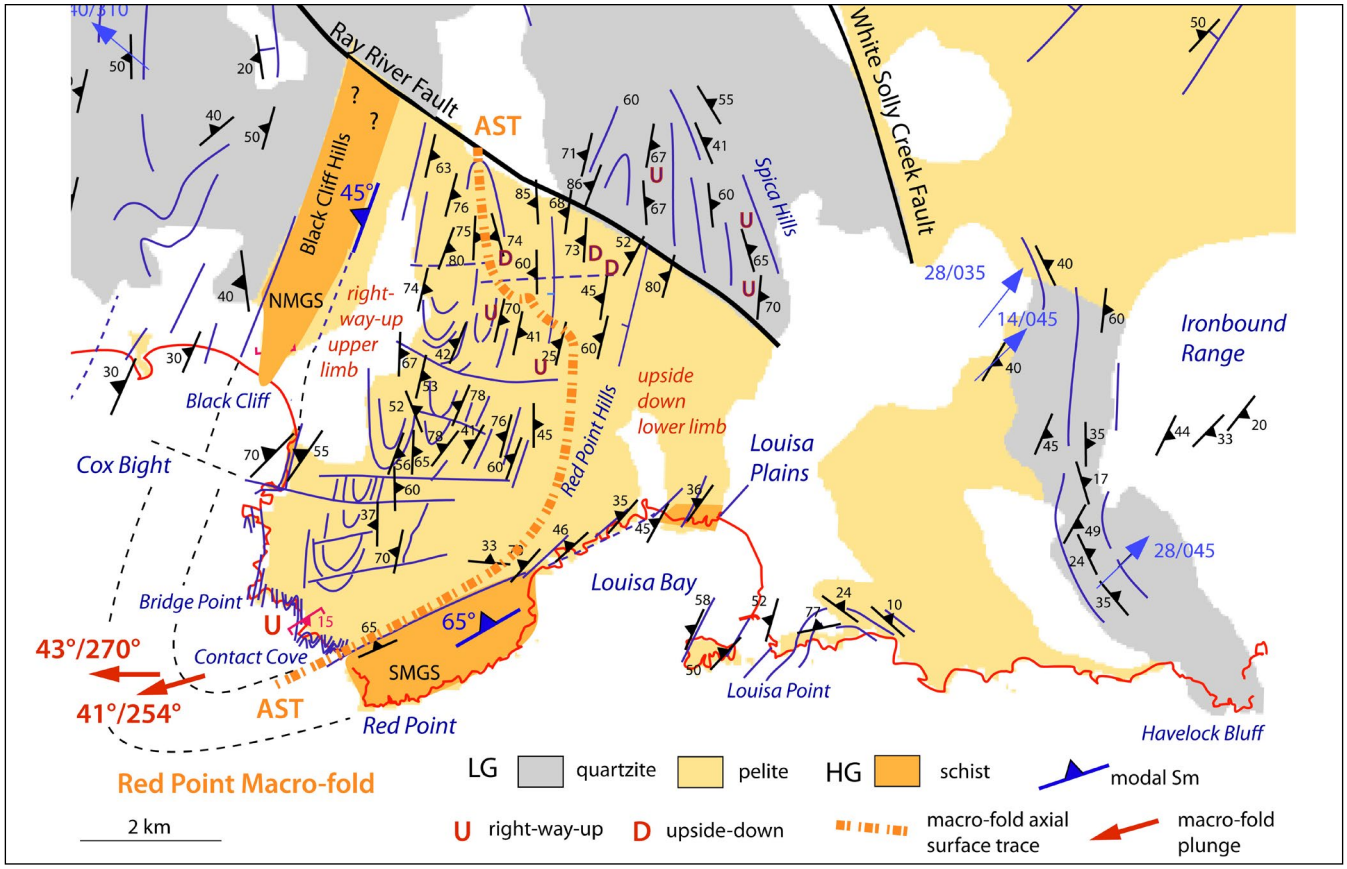

Figure 16. Structure map of the Red Point macro-isoclinal fold. Structural data from 1) Lennox (2013) based on mapping in January-February of 1980, and 2) Mulder (2013) Honours thesis mapping. Younging data from Lennox (2013) plotted as D: upside down compositional layering; U: right-way-up compositional layering. Blue arrows: lineation Lm attitude data. Lithological map base is from Mineral Resources Tasmania 1:250000 digital atlas series. Thin dashed black lines depict the macro-fold closure. The thick orange dashed line is the macro-fold axial surface trace (AST). NMGS: Northern medium grade sequence; SMGS: southern medium-grade sequence.

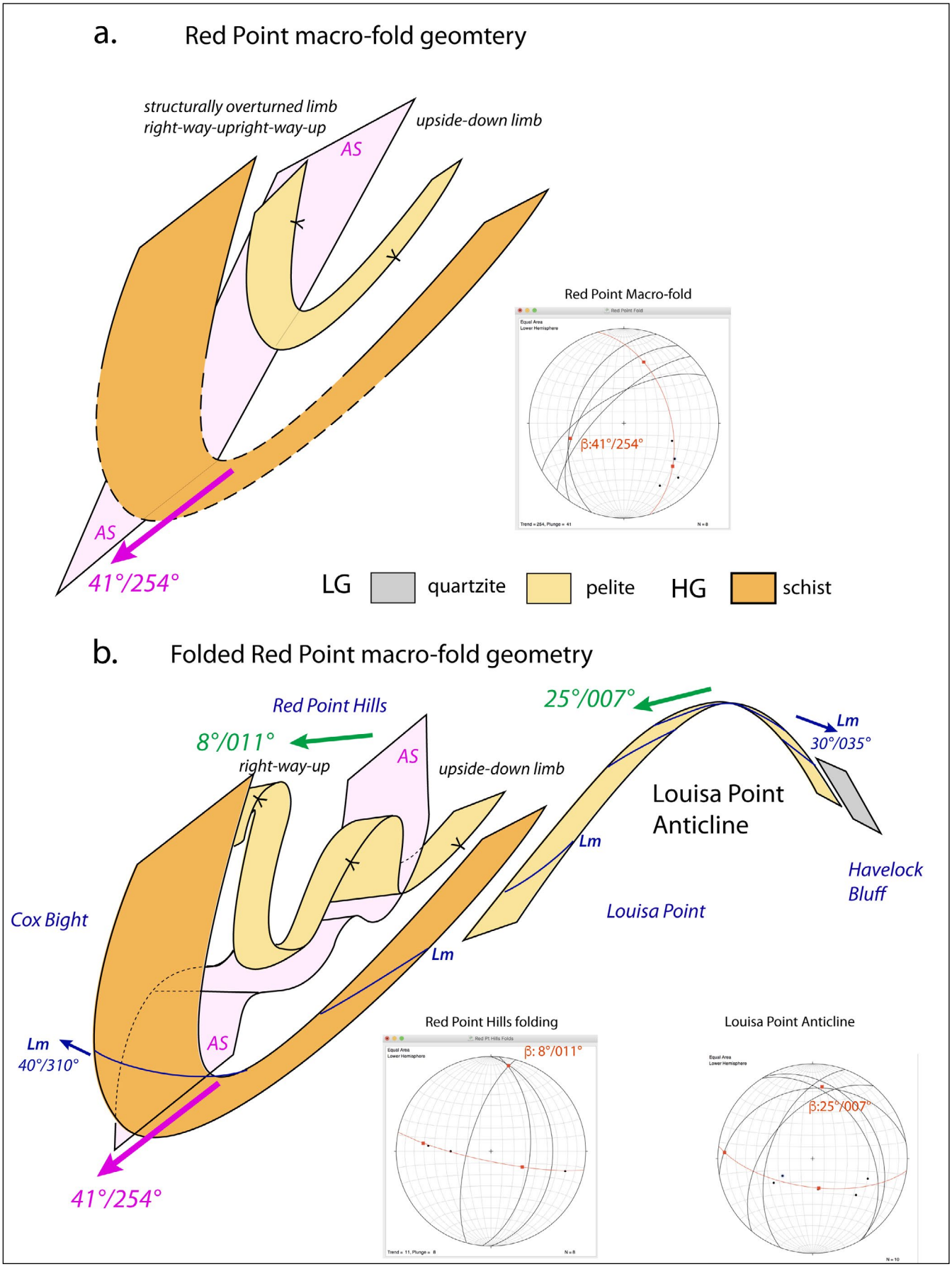

Figure 17. Interpretative 3D structural geometry of the Red Point Hills-Red Point area.

a) Macro-fold form interpreted by connecting the northern and southern HG belts by an inclined plunging closure with a β axis of 41°/254° (stereonet inset). b) 3D schematic geometrical diagram of a refolded Red Point macro-fold by younger north-south folding in the Red Point Hills and the Louisa Bay-Louisa Point area. The east-west-trending, right lateral strike slip-faults have been removed in 3D diagram. Stereonet insets show the β fold axis determinations in the Red Point Hills folding (β: 8°/011°) and the Louisa Point Anticline (β: 25°/007°).

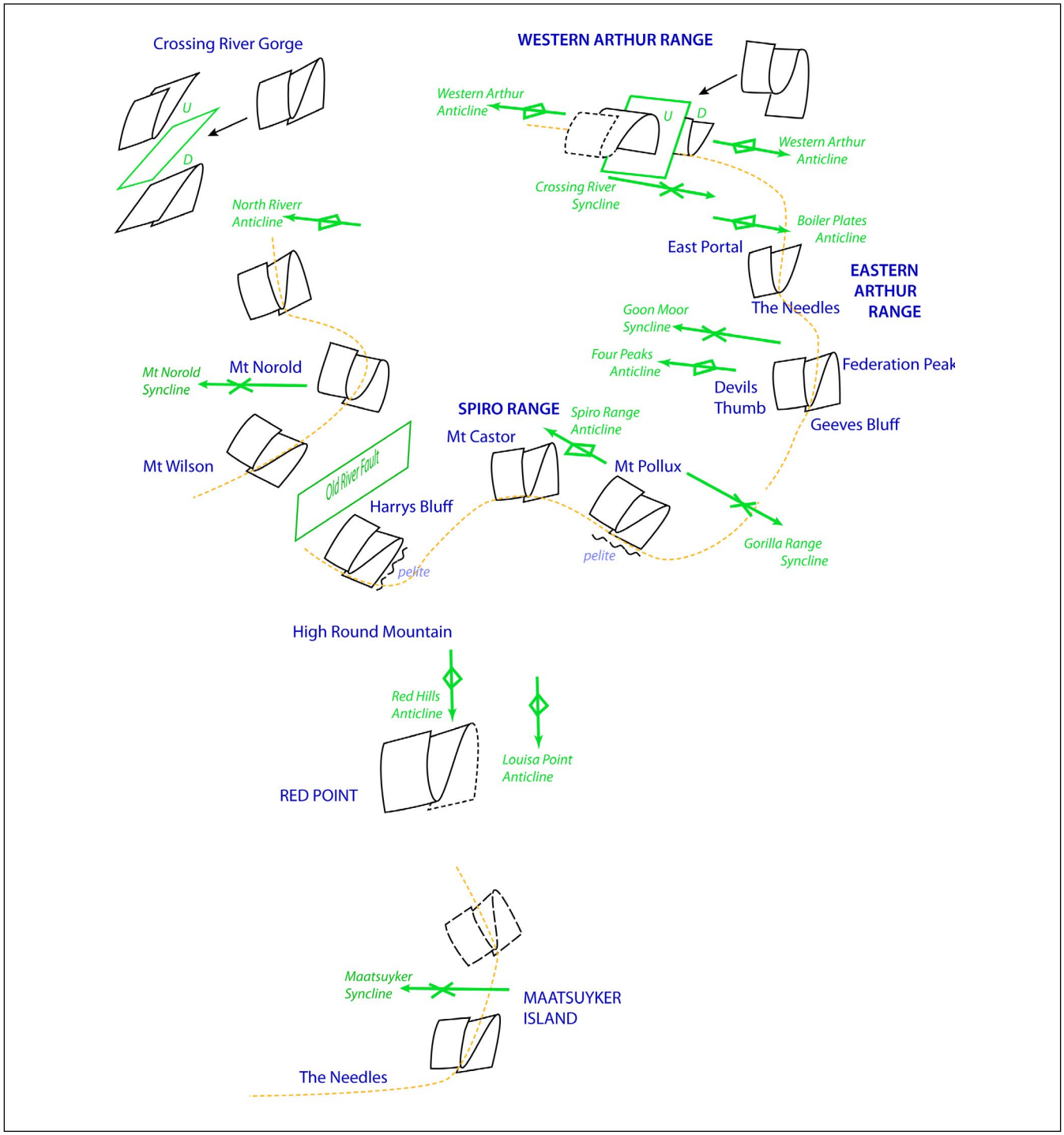

Figure 18. Schematic asymmetric fold-pair diagram showing the 3D geometry and attitude of the S-vergence (down-plunge) fold pair across the eastern Southern Tyennan domain. The spatial positioning reflects an approximate geographic base. Geographic location names are in blue text. Younger, Devonian fold axial surface traces and faults are shown in green and with labeling in green text. The orange dashed line connects the hinge-lines of the structurally higher south-closing macro-isocline across the region.

Length scales are ~60 km from the northern end of the Western Arthur Range in the north to Maatsuyker Island in the south, and ~20 km from Mt Wilson-Mt Norold in the west to Federation Peak in the east.

3.3.2 Profile Construction and Description

Construction of four regional profiles (Figure 19) utilising the positions, geometry and approximate fold attitudes of the folds exposed in hillsides shows that the 3rd order folds are part of a repeated, asymmetric, S-vergent fold couple that define a "wave-train" constrained to a particular structural level and crops out in the exposed landscape with about 1000 m of relief (Figure 19). The fold couple itself consists of a structurally higher, southwest-closing isoclinal hinge linked to a structurally lower, northeast-closing hinge. This repeated pattern is shown through hillsides intersecting the fold "wave-train" (Figures 18 and 19). It extends from the Eastern Arthur Range in the northeast to Mt Norold in the middle part of the region. As shown in the 3D fold geometry diagram (Figure 18) the fold pair and the linking fold "wave-train" are broadly warped by the younger, open Devonian fold sets (Figure 19).

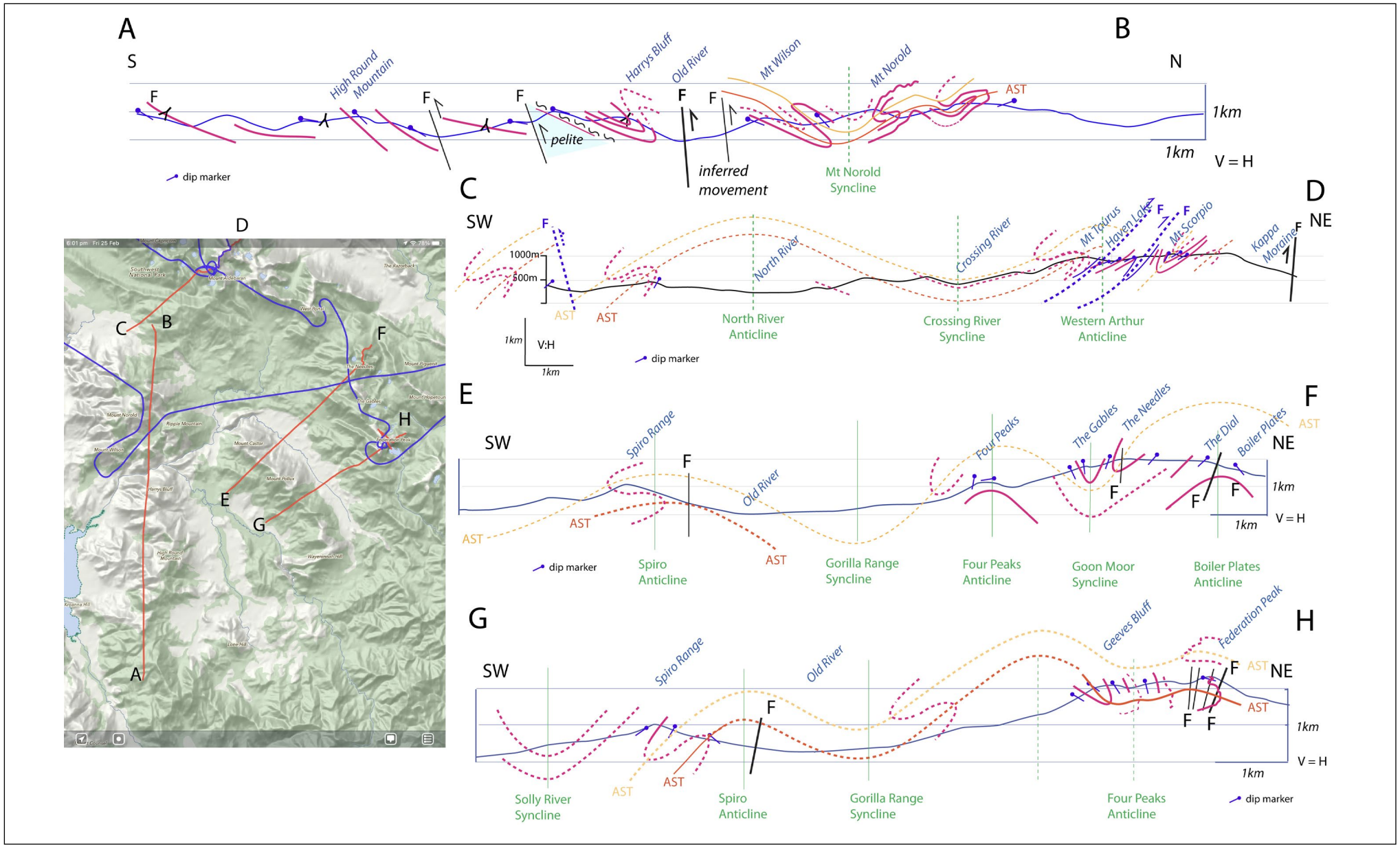

Figure 19. Structural profiles across the eastern Southern Tyennan domain. Section A-B' north-south profile from Mt Norold to High Round Mountain. Section C-D: southwest-northeast profile from Mt Norold to Mt Scorpio and Kappa Moraine. Section E-F: southwest-northeast profile from the Boiler Plates to the Spiro Range. Section G-H: southwest-northeast profile from Federation Peak to the Spiro Range. The blue line traces are the helicopter flight paths during the 2020 flight.

1. **Profile A-B** is a north-south profile extending from High Round Mountain in the south to Mt Norold in the north (Figure 19). The northern part of the section from Mt Wilson to Mt Norold shows three oblique intersections of the early, isoclinal, asymmetric fold pair folded about the younger, open Mt Norold Syncline. The fold profile construction shows the fold pair has an apparent ~600-700 m wavelength from upper long limb-to-lower long limb. To the south a series of east-west trending, high-angle, oblique slip reverse faults with north block-up sense truncate and offset the fold pair. At Harrys Bluff south of, and in the immediate footwall to, the Old River Fault the cliff exposure projections combined with mapping show the regional asymmetric fold pair transitional into a high-strain platy quartzite overlying pelite in the hanging wall to another reverse fault. Younging data from Harrys Bluff and High Round Mountain (Lennox, 2013) show that the quartzite in the High Round Mountain ridgeline to the Ray Range is right-way-up and sits at the common limb of the fold pair. A series of north-side-up reverse faults repeat the limb segment such that it occurs at approximately the same structural level along the ridgeline.

2. **Profile C-D** extends from the North River headwater valley across the Western Arthur Range to Mt Scorpio (Figure 19). The profile has limited structural data at the south west end of the profile but has the detailed Mt Taurus-Mt Scorpio section (Gray and Vicary, 2022a, fig. 49) at the northeast end. The middle part of the profile is dominated by the younger, broad, open Devonian folds of the North River Anticline and the Crossing River Syncline. Projecting the axial surface traces of the fold pair across the younger syncline-anticline pair gives the inferred position of the fold pair south of the North River valley. A similar level to that of the fold pair in the Mt Norold ridgeline requires the presence of a high-angle, north-side-up, reverse fault cutting the southwest flank of the North River Anticline (Figure 19).

3. **Profile E-F** extends from the north end of the Spiro Range to the Boiler Plates at the north end of the Eastern Arthur Range (Figure 19). The north end of the profile is based on the detailed Boiler Plates-Goon Moor profile (Gray and Vicary, 2022a, fig. 64). Axial surface trace projection of the fold pair across the younger, open Devonian folds including the Gorilla Range Syncline, the Four Peaks Anticline, the Goon Moor Syncline and the Boiler Plates Anticline requires the uppermost south-closing hinge at Mt Castor in the Spiro Range to match the projected hinge to the Needles in the Eastern Arthur Range.

4. **Profile G-H** extends from Mt Pollux in the Spiro Range through Geeves Bluff to Federation Peak at the east end of the Eastern Arthur Range (Figure 19). The northeast end of the profile is based on the more detailed Geeves Bluff-Federation Peak profile (Gray and Vicary, 2022a, fig. 75). Axial surface projection of the structurally lower, northeast-closing hinge from Mt Pollux across younger, open Devonian folds including the Spiro Range Anticline, the Gorilla Range Syncline and the Four Peaks Anticline suggest that the northeast-closing hinge exposed from Geeves Bluff to Federation Peak is part of the same fold train.

3.4 Mineral Lineation Lm and Fold Axis (FA) Relationships

The lineation Lm and the early isocline fold axis (FA) patterns, as well as the relationships between them (Figures 20, 21 and 22), provide geometrical constraints regarding the overall macro-fold geometry. Parts of the data are difficult to explain and may be due to mixing of the fold axis data of the younger fold sets with younger crenulation lineation data. At this stage there is no way to verify this as these data were obtained from the early BHP mapping (Hall, 1965).

3.4.1 Mineral Lineation Lm Orientation Pattern

The mineral/stretching lineation (Lm) orientation pattern is highlighted by the thick blue lines on Figure 20. North of the Ray River Fault the lineation Lm pattern is dominantly southwest-trending for the central part of the eastern Southern Tyennan domain. Changes occur in the Arthur Range that can be geometrically explained by isoclinal folding of the early lineation Lm about a macro-fold axis of 25°/270° (Gray and Vicary, 2022a, fig. 48d). South of the Ray River Fault changes in the Lm pattern from northwest-trending to northeast-trending can also be geometrically explained by isoclinal folding of the lineation by the Red Hills macro-fold about a fold axis of 42°/270°. The change in orientation to more north-south trending along the Rugby Range may also relate to isoclinal folding (F2) as part of an early fold hinge captured as the western trailing hinge of the Mt Braddon mushroom fold interference pattern.

3.4.2 Fold Axis Orientation Pattern

The early isocline fold axis pattern is highlighted by the thick pink lines in Figure 21.

Throughout most of the eastern Southern Tyennan domain the early isocline fold axes are consistently east-west trending.

3.4.3 Early Isocline Fold-Hingeline Vergence Pattern

Rotation relationships of the early isocline fold axis towards the lineation are shown by the red-curved arrows with either clockwise and anticlockwise rotation sense (Figure 22). Most of the eastern Southern Tyennan domain has anticlockwise fold-hingeline vergence (Figure 22). This rotation sense supports the inferred structural position of 1) on the lower limb of the De Witt-Propsting mega-sheath fold, and 2) on the southern side of the De Witt-Propsting mega-sheath fold medial line, that is the geometrical line through the centre of the Davey River fold system sheath nose (Gray and Vicary, 2022b).

Rotation sense changes also occur across the early macro-isocline hinges in the Arthur Range (Figure 22).

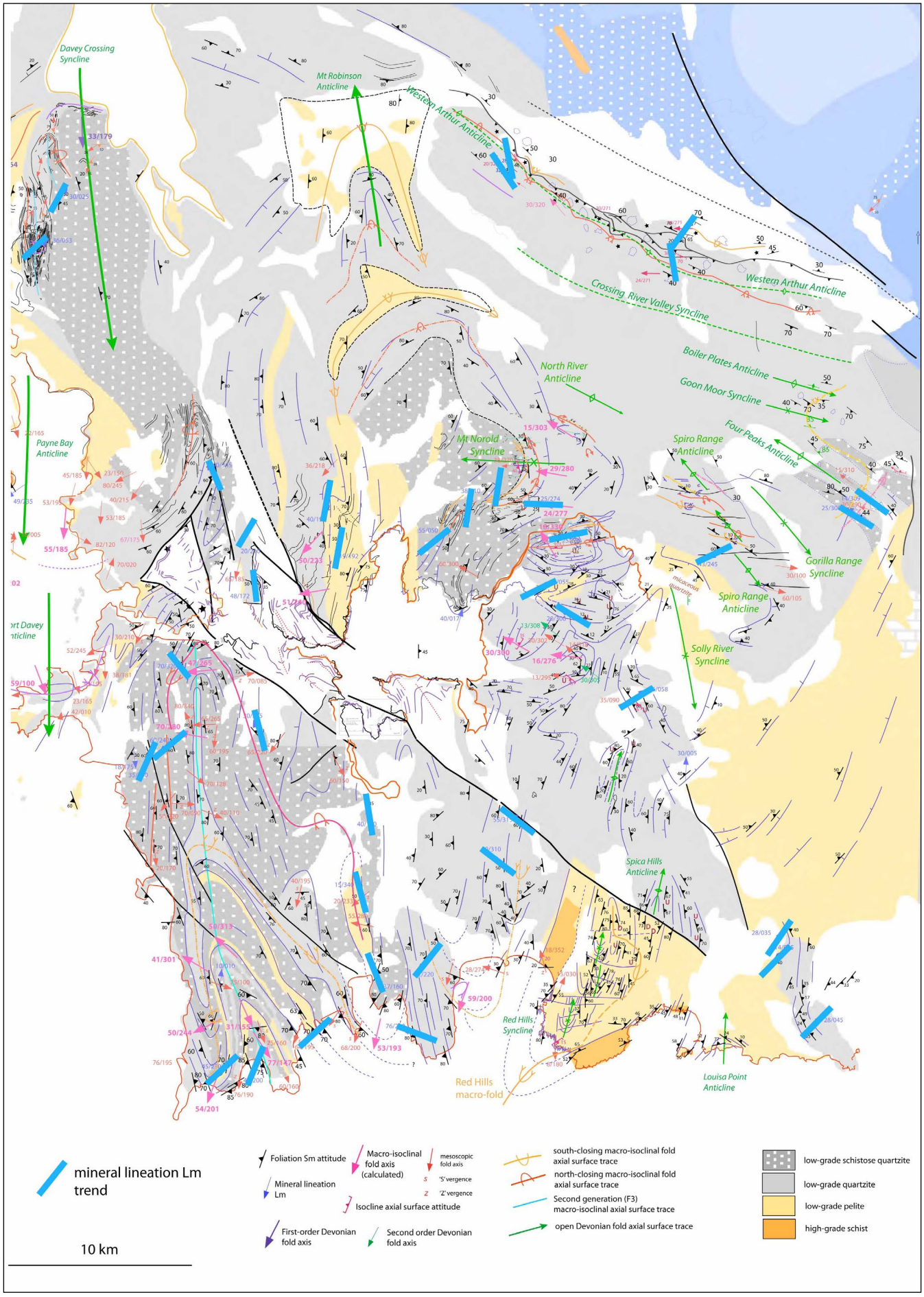

Figure 20. Mineral lineation (Lm) trend map with mineral lineation plunge directions highlighted by the thick blue line traces on Mineral Resources Tasmania 1:250000 digital atlas lithological base.

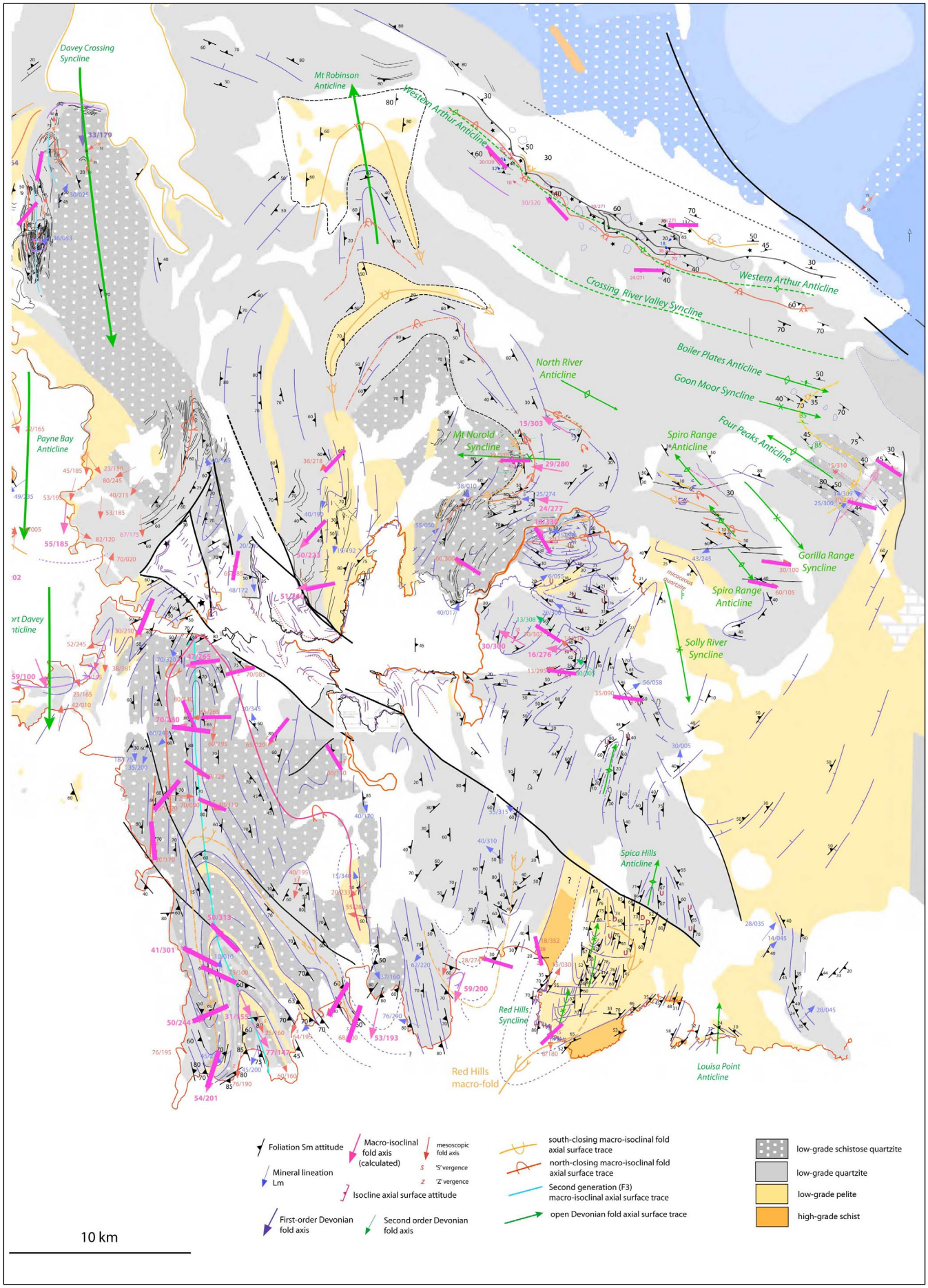

Figure 21. Early isocline fold axis (FA) trend map with mesoscopic-fold plunge directions highlighted by the thick pink line traces on Mineral Resources Tasmania 1:250000 digital atlas lithological base.

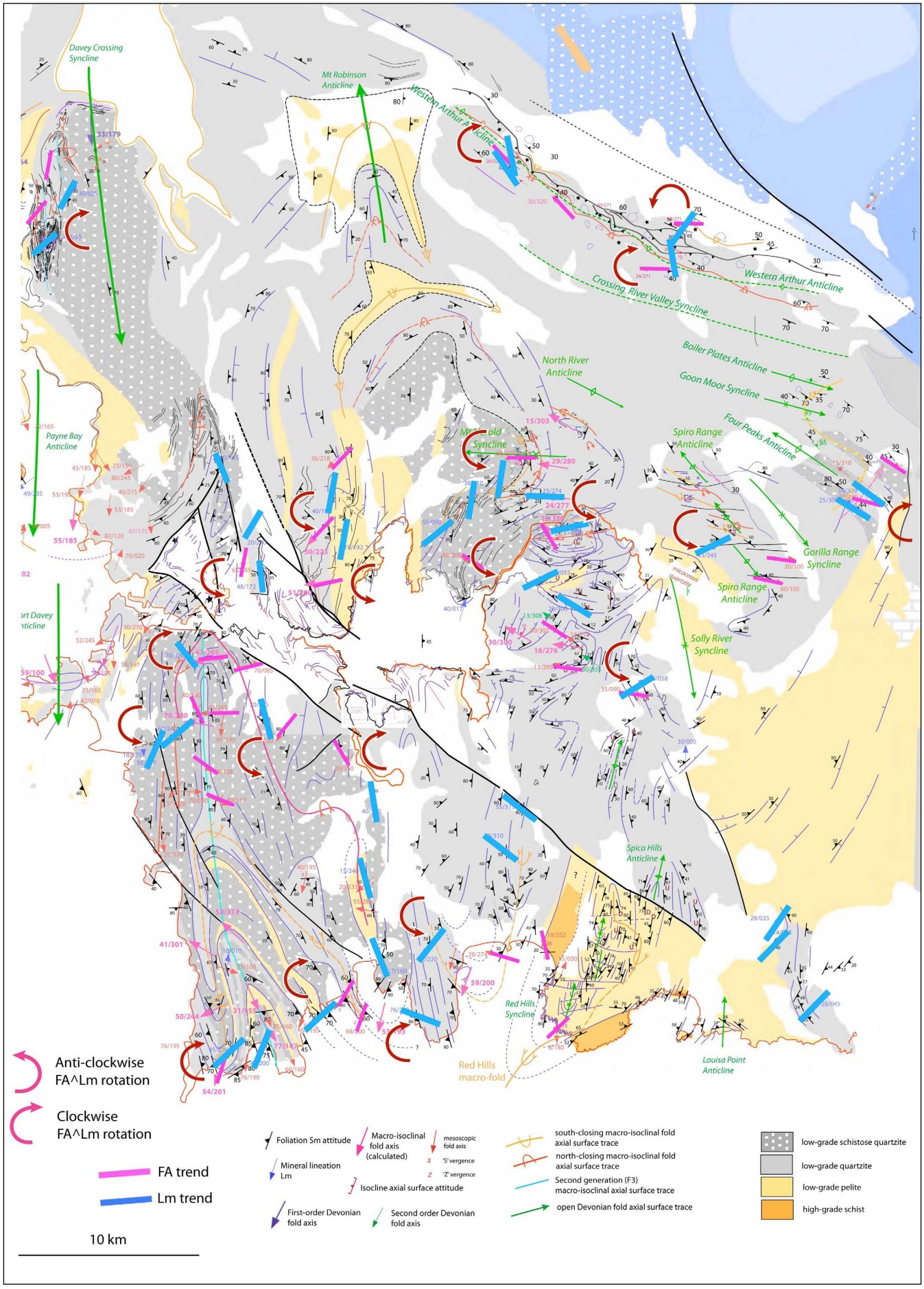

Figure 22. Fold-hingeline vergence map showing Fold axis (FA) to lineation (Lm) rotation by the red-curved arrows.

4.0 DETAILED STRUCTURAL GEOLOGY OF THE EASTERN PART OF THE SOUTHERN TYENNAN DOMAIN

Maps, sections and photographs are provided in this section to provide the detail and basis of the eastern Southern Tyennan domain structural overview in the previous section. The structure at each geographic location (Figure 2) is described and discussed.

4.1 Arthur Range

The Arthur Range lies in the northeast corner of the Southern Tyennan domain and consists of the Western and Eastern Ranges (Figures 2 and 3). Details of the structural geology of the Arthur Range are presented in Gray and Vicary (2022a) with a synopsis presented here.

Stacked ridge profiles for both the Western (Figure 23) and Eastern Arthur Range (Figure 24) show a fold-pair of regional-scale, Cambrian recumbent-isoclinal macro-folds, with a structurally higher southwest-closing closure overlying a structurally lower northeast-closing closure. The spine of the Western Arthur Range consists of a major northeast-closing recumbent macro-fold that extends the length of the range (~21 km) and is folded by the younger open Western Arthur Anticline (Figures 4 and 18). An oppositely, southwest-closing recumbent fold sits in the footwall to the Devonian reverse fault system along the north flank of the range (Figure 23).

The northeast flank of the Arthur Ranges is defined by a Devonian reverse fault system that truncates and offsets these Cambrian recumbent folds (Figures 4 and 23). The faults are associated with a sub-parallel series of open, upright northwest-trending Devonian folds that swing to a more east-west trend towards the eastern end of the Western Arthur Range. Spacing of the Devonian axial surface traces is on the order of ~1.5 km. This younger folding refolds the older Cambrian large-scale recumbent folds that are also northwest-trending. These relationships are shown in regional profile C-D (Figure 19).

The Eastern Arthur Range shows two structural levels through the fold pair with 1) the northern ridgeline profile (Boiler Plates to Goon Moor) exposing the structurally higher southwest-closing fold hinge, and 2) the southeastern ridgeline (Federation Peak to Geeves Bluff) exposing the structurally lower northeast-closing fold hinge (Figure 24). These relationships are shown in regional profiles E-F and G-H (Figure 19).

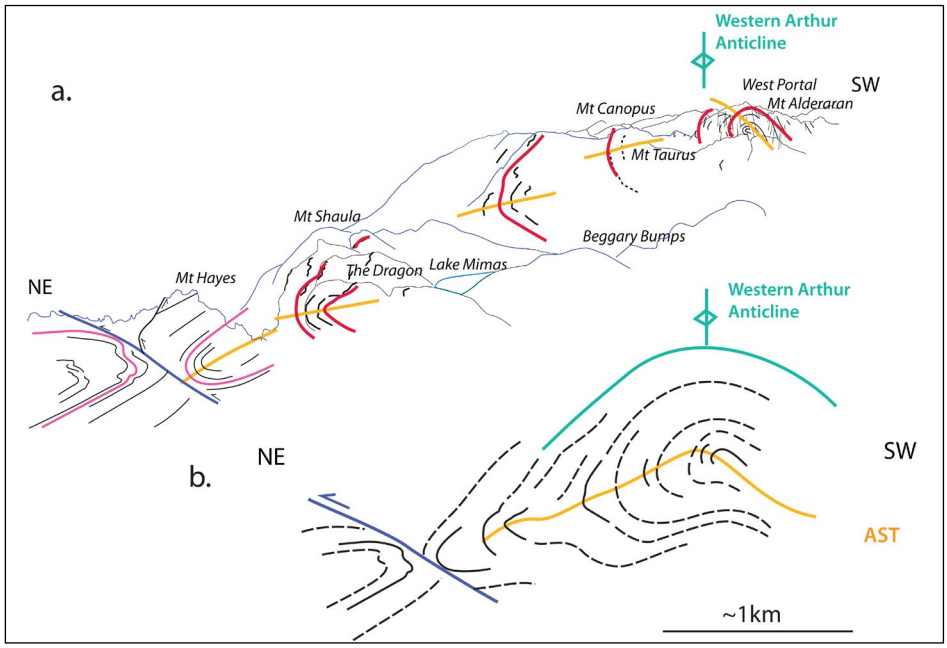

Figure 23 (left). Western Arthur structural profile. a) Stacked ridge profiles through the Western Arthur Range from Mt Hayes to Mt Aldebaran producing a composite structural profile at the leading edge of the Southern Tyennan domain. Through the profile there is an apparent layering change from thicker bedded quartzite in the outer part of the hinge, noticeable particularly at Mt Hayes (Gray and Vicary, 2022a, fig. 17), to thinner bedded quartzite through the core of the northeast-closing fold, noticeable in the Mt Columba-The Dragon-Dorado Peak profile (Gray and Vicary, 2022a, fig. 22). b) Simplified structural profile based on the ridge exposures in (a) showing the northeast-closing macro-isoclinal fold that dominates the Western Arthur ridge crest. orange line: axial surface trace of the recumbent macro-isocline.

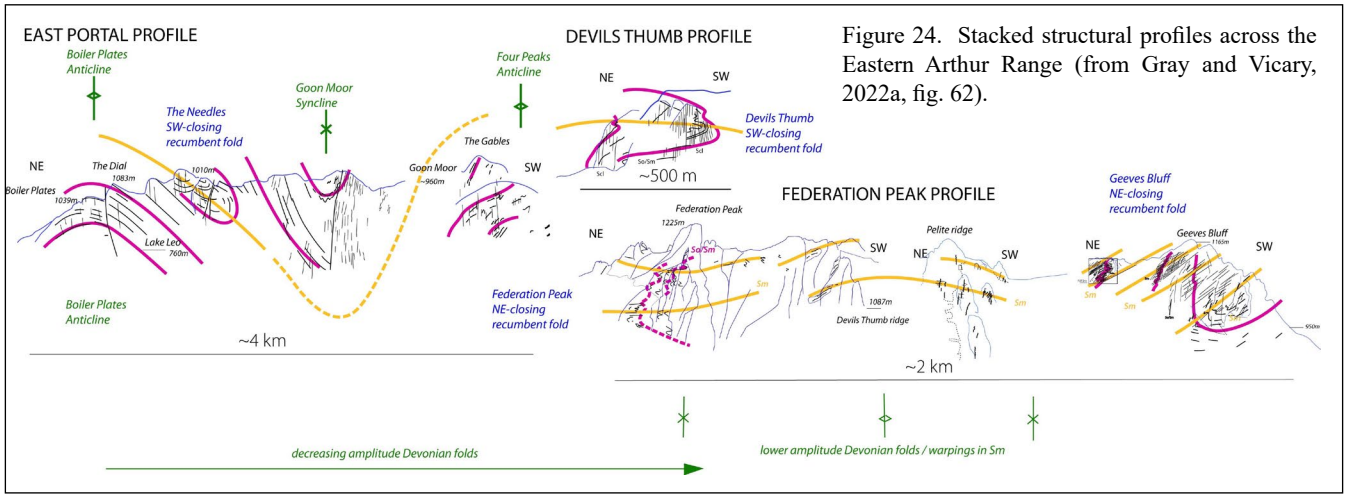

Figure 24. Stacked structural profiles across the Eastern Arthur Range (from Gray and Vicary, 2022a, fig. 62).

4.2 Spiro Range

The Spiro Range is an isolated northwest-trending ridgeline in quartzite separated from, but sub-parallel to, the Devils Thumb-Thwaites Plateau quartzite ridge coming off Federation Peak (Figure 3).

Interpretation of oblique ridgeline photographs taken from a helicopter (Figures 5, 25 and 26) indicates that the Spiro Range, like the Arthur Range consists of a macro-fold pair of southwest- and northeast-closing, recumbent isoclinal macro-folds. This fold-pair has been truncated and offset east-west trending, sinistral-oblique slip faults (Figure 25b). Profiles E-F and G-H (Figure 19) are sections through the Spiro Range.

4.3. Harrys Bluff and High Round Mountain

The Harrys Bluff-High Round Mountain ridge is part of a ridgeline cut by the Old River extending through Mt Wilson to north of Mt Norold (Figure 27). It is dominated by east-west trending, west plunging, younger, open Devonian folds and that fold early isoclinal macro-folds that are on the flanks of the ridge (Figures 12 and 27). East-west high-angle reverse faulting is also common, as well as the major, larger throw Old River that fault juxtaposes the isoclinal macro-fold pair at Mt Wilson in the up-thrown block against the fold pair exposed in Harrys Bluff in the downthrown block (section A-B, Figure 19).

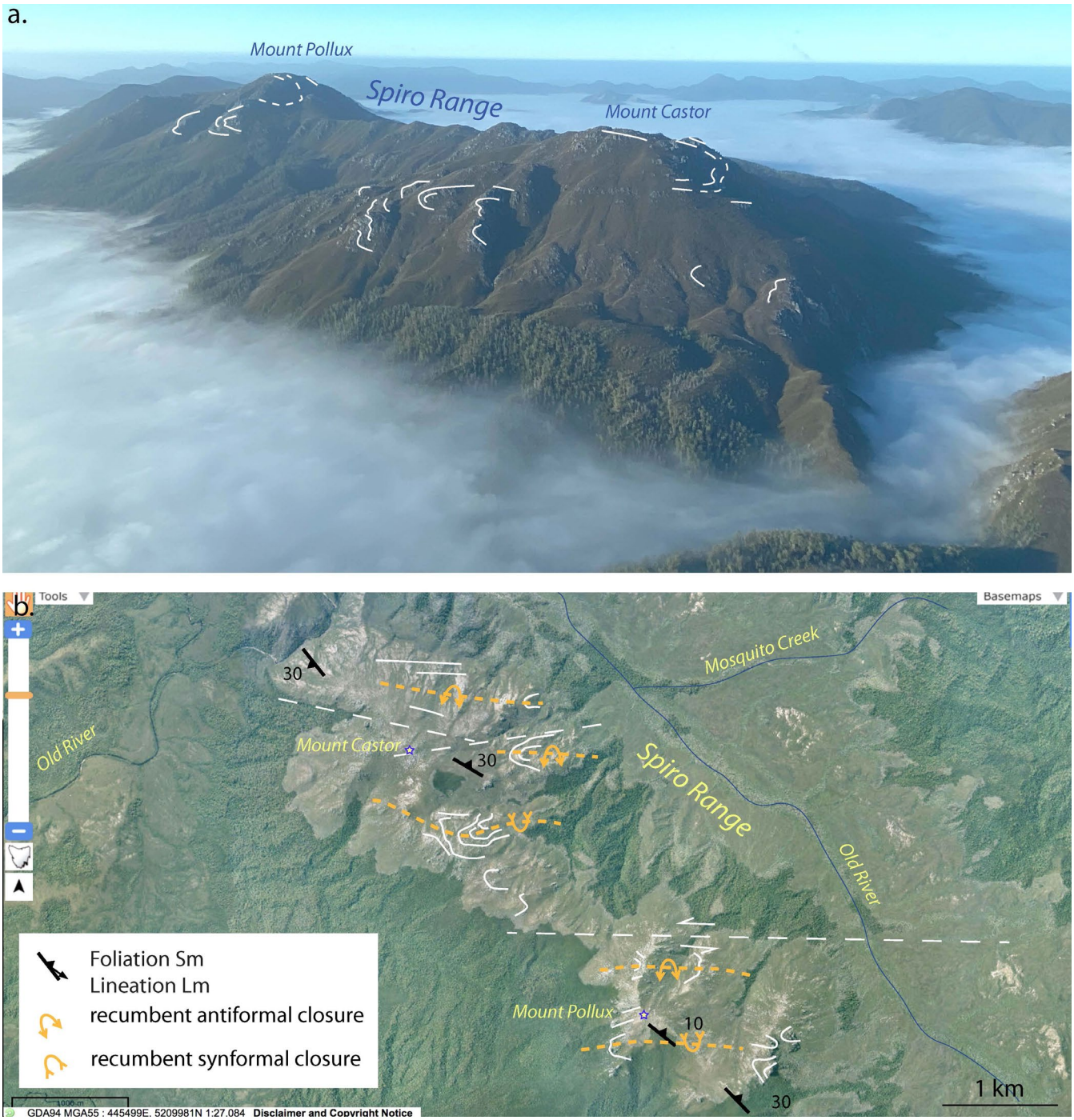

Figure 25. Structural relationships of the Spiro Range. a) Aerial view along the range showing Mt Castor and Mount Pollux and white formlines in the dominant layering (So/Sm). b) ListMap Aerial photograph of the Spiro Range with structural geological data and relationships. white lines: formlines in So/Sm; white dashed lines: fault traces; orange dashed lines: fold axial surface traces.

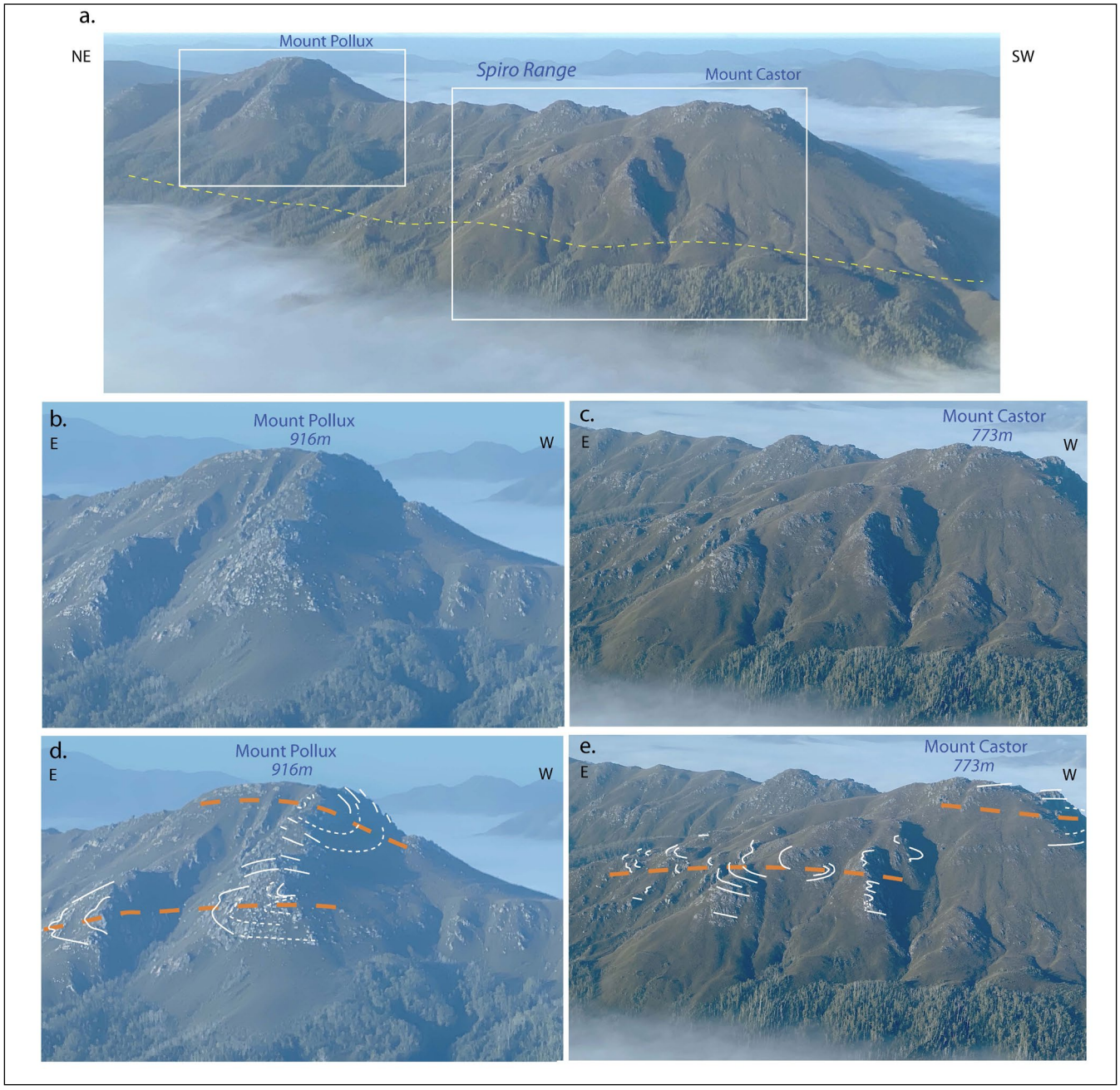

Figure 26. Aerial views of the Spiro Range looking to the south-southeast. The flight path of the helicopter was southwest along the Old River Valley towards Bathhurst Harbour. a) Spiro Range with white boxes highlighting the enlarged views below. b) Mount Pollux. c) Mount Castor. d) and e) formline interpretation of Mount Pollux and Mt Castor respectively. *White lines: formlines in So/Sm; dashed orange line axial surface traces of southwest- and northeast-closing, recumbent isoclinal macro-folds. Blue lines: fault traces.*

Mapping by Taylor (1959), Hall (1965) and Williams in 1980 (Lennox, 2013) suggested that the quartzite overlies pelite with a schistose quartzite along the contact (Figures 19 and 28). Bounded by the Old River on the north and the Solly River on the east, the northern and north-eastern faces of Harrys Bluff provide oblique structural profiles showing a major southwest-closing recumbent isoclinal macro-fold (Figures 29) and in the lower part of the northeast cliff face there is a suggestion of northeast-closing recumbent fold cut by zones of more intense foliation (Figure 30). The northeast face also provides ~680 m section through the quartzite (Figure 30).

High Round Mountain and the Ray Range occur 1) on the lower limb of the major Harrys Bluff recumbent fold and 2) have cross-bedding occurrences indicating right-way-up (Lennox, 2013) (section A-B, Figure 19).

The map (Figures 27 and 28) shows interference between east-west trending open folds (green dashed axial surface traces) and the recumbent isoclinal macro-folds (orange dashed axial surface traces). Many of the east-west folds are asymmetric undulations in NW- dipping So/Sm that defines the limbs of isoclinal macro-folds (section A-B, Figure 19). This contrasts with the northern ridge segment at Mt Norold where a more open, upright east-west syncline dominates (Mt Norold Syncline in section A-B, Figure 19).

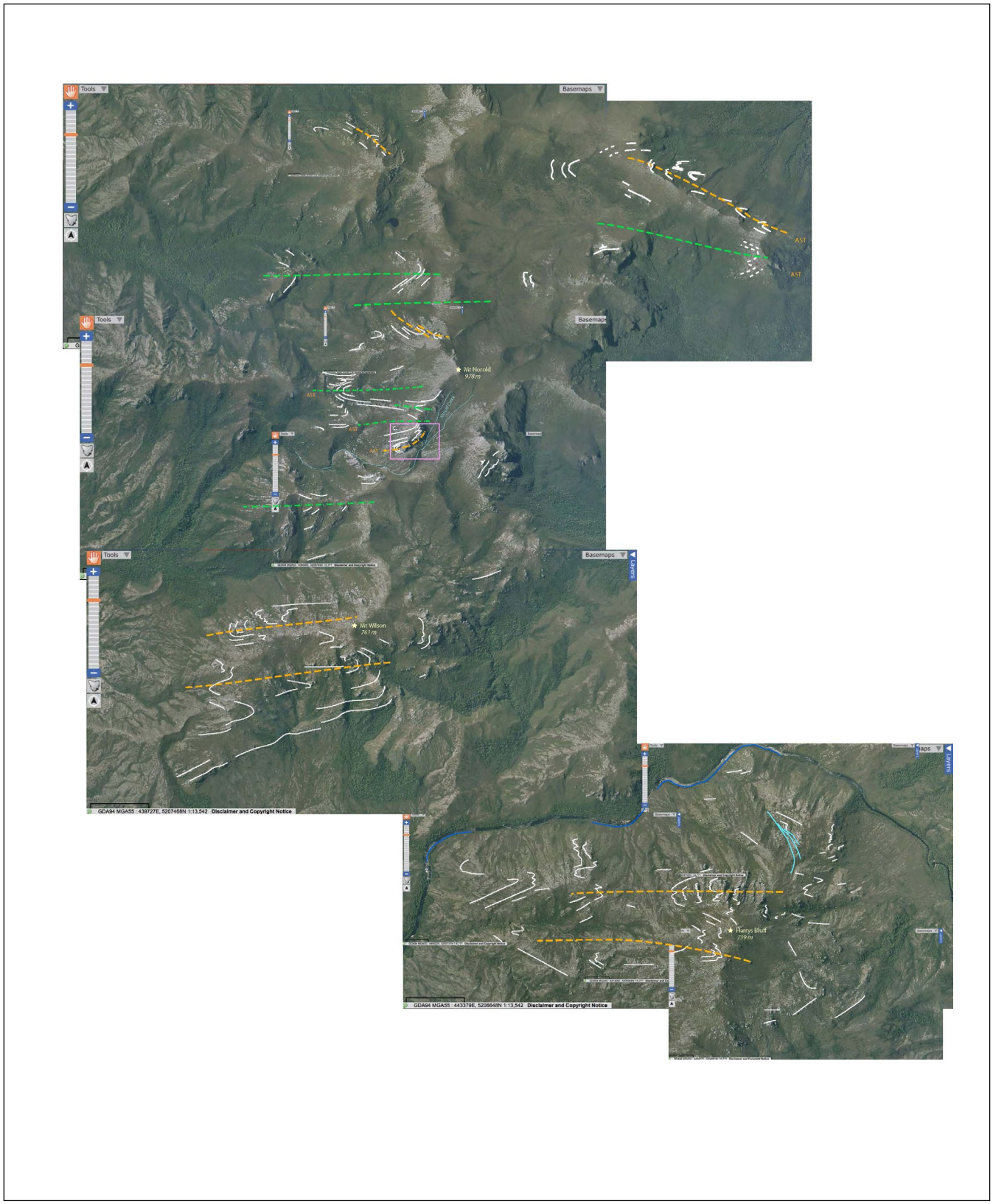

Figure 27. Structure map of the Harrys Bluff-Mt Wilson-Mt Norold region of the eastern part of the Southern Tyennan domain. Made up of individual stitched ListMap airphotos, these represent parts of the region shown in more detail in Figures 28, 38, 32 and 35. Formlines in So/Sm (white line traces) have been interpreted from ListMap aerial photographs. *Orange dashed line traces: early isoclinal macrofold axial surface traces. Green dashed line traces: younger Devonian open fold axial surface traces.*

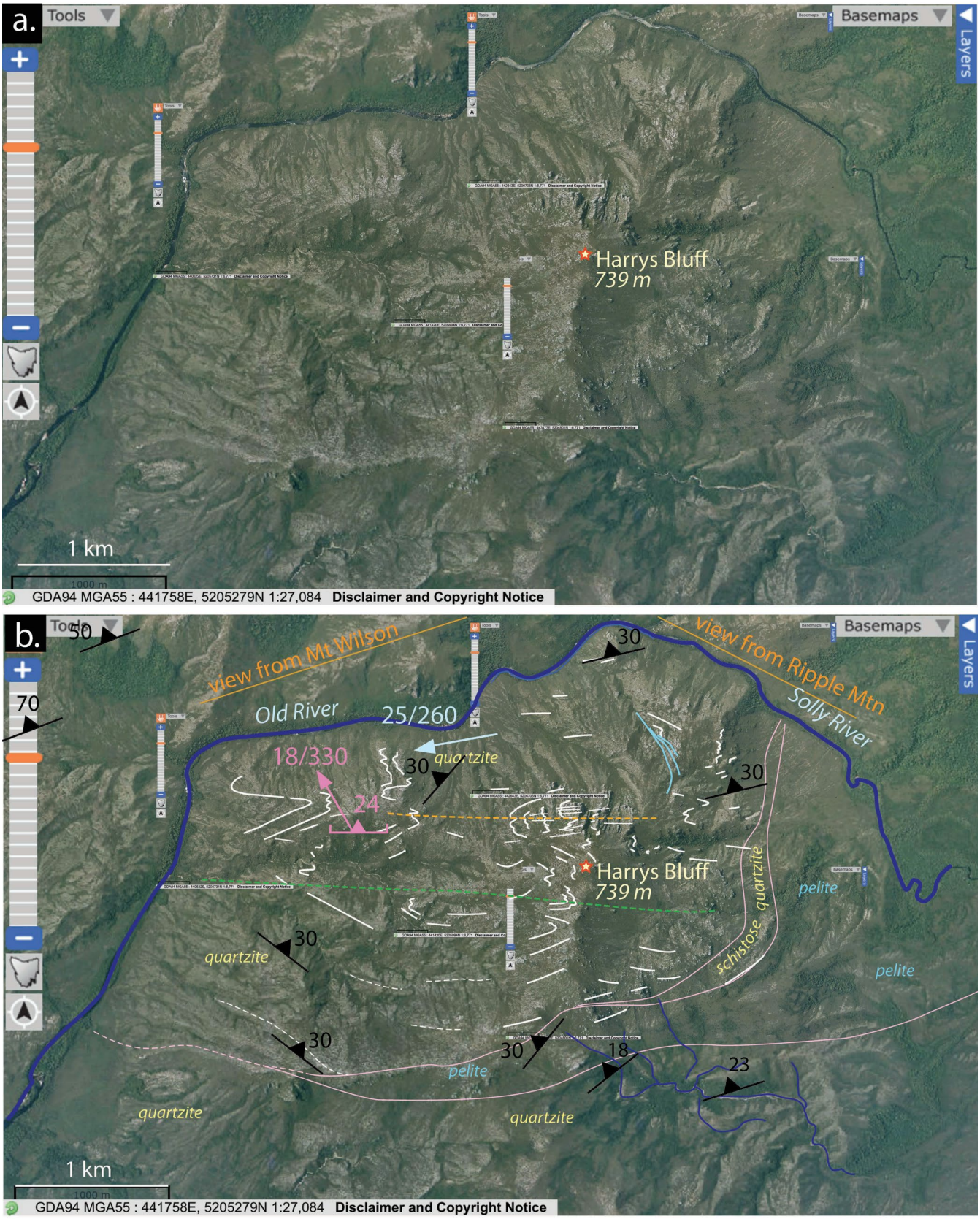

Figure 28. Structure map of Harrys Bluff (739 m elevation) with stitched ListMap Google satellite image as base. The ovoid-shaped outcrop pattern centred on Harrys Bluff relates to the intersection of the lowermost southwest-closing, northwest-plunging (18°/330°) recumbent fold and open, gently plunging east-west folds that warp the with the Bluff topography.

So/Sm formlines: white line traces. Litho-tectonic unit contacts: pink line traces. Recumbent fold axial surface trace: orange dashed line trace. East-west open fold axial surface: green dashed line trace. Blue lines are brittle fault traces.

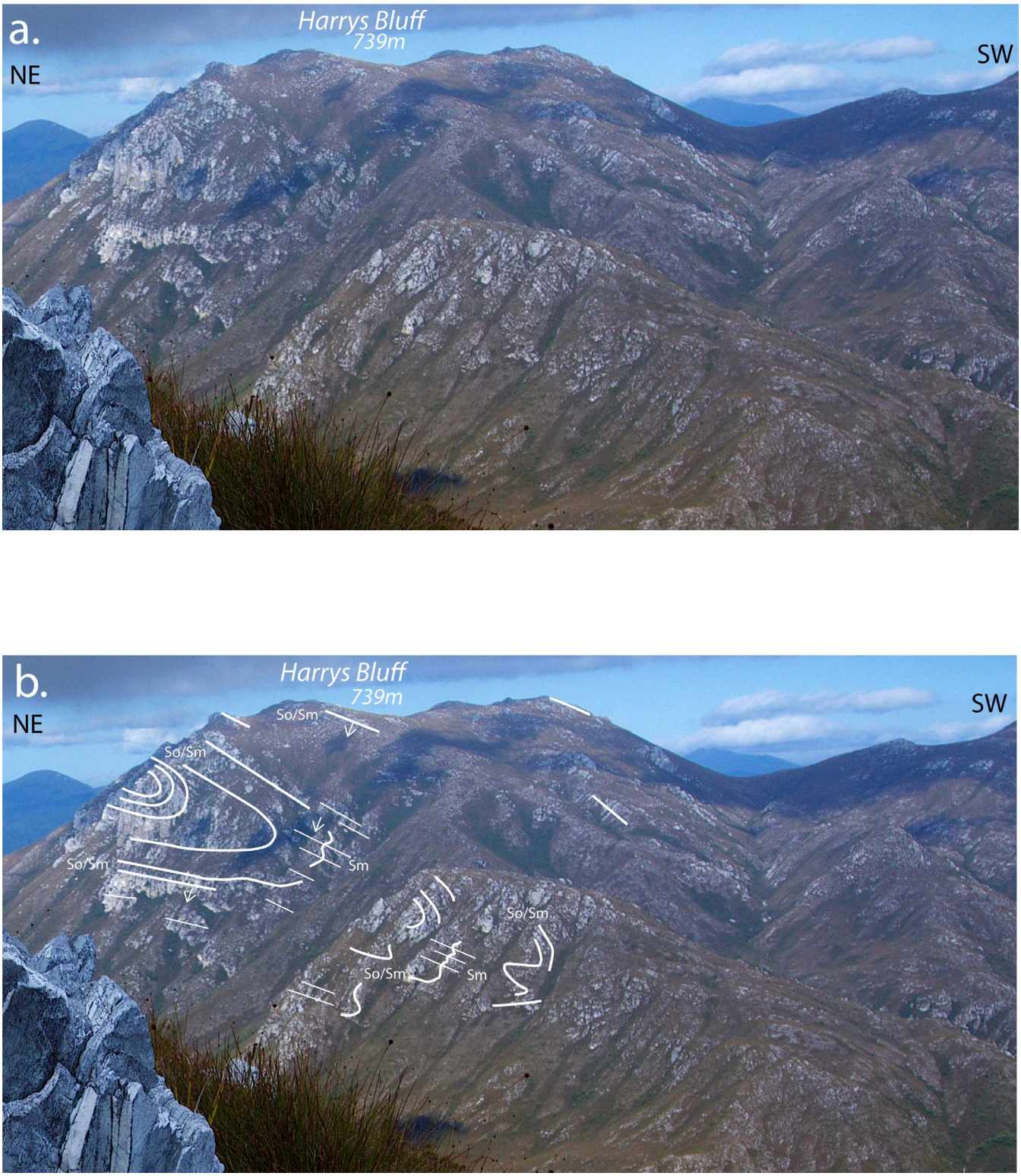

Figure 29. Approximate profile view of Harrys Bluff southwest-closing recumbent isoclinal fold. View to the southeast from Mount Wilson. Formlines are apparent dip traces on the Bluff cliff faces with So/Sm dipping towards the lower right into the Old River valley. The fold hingeline is plunging towards the camera with both recumbent fold limbs dipping to the northwest. The white arrows indicate dip directions of Sm and So/Sm in the plane of the photograph. Photo credit: Beccalunnon, RockMonkeyAdventures.

Figure 30. Harrys Bluff from Ripple Mountain showing quartzite apparent thickness of ~690 m with oblique view of the southwest-closing recumbent isocline in the upper cliff face. The photo shows the recumbent fold upper limb eroded away with the lower limb projected across High Round Mountain (photo top left). There is suggestion of a northeast-closing recumbent fold in the vegetated lower part of the Bluff (left side of photo). The dashed line (lower left) is the interpreted contact with the underlying schist/phyllite (pelite). Photo credit: Beccalunnon, RockMonkeyAdventures.

4.4 Mt Wilson

Mt Wilson (Figures 27 and 31) is dominated by a south-closing, recumbent, isoclinal macro-fold contained within north-dipping quartzite So/Sm (Figure 7). The recumbent fold-hinge is exposed on the north flank of Mt Wilson (Figure 7 and orange dashed line in Figure 31) with the lower limb on the south flank folded by open east-west trending folds (green dashed lines in Figure 31). This is the same fold as that exposed on the north face of Harrys Bluff, but offset and on the up-thrown block of the Old River Fault (section A-B, Figure 19).

The north face of Mt Wilson exposes a west-closing recumbent fold with the right-way-up lower limb exposed to the south refolded by east-west trending open folds (dashed green lines as axial surface traces). Way-up is based on younging in quartzites at Richea Peak along strike (based on photo interpretation RockMonkeyAdventuresTM photograph). The recumbent-fold lower limb consists of strongly and multiply deformed quartzite (Figure 7) showing transposition layering development and multiple crenulation cleavages (Scc).

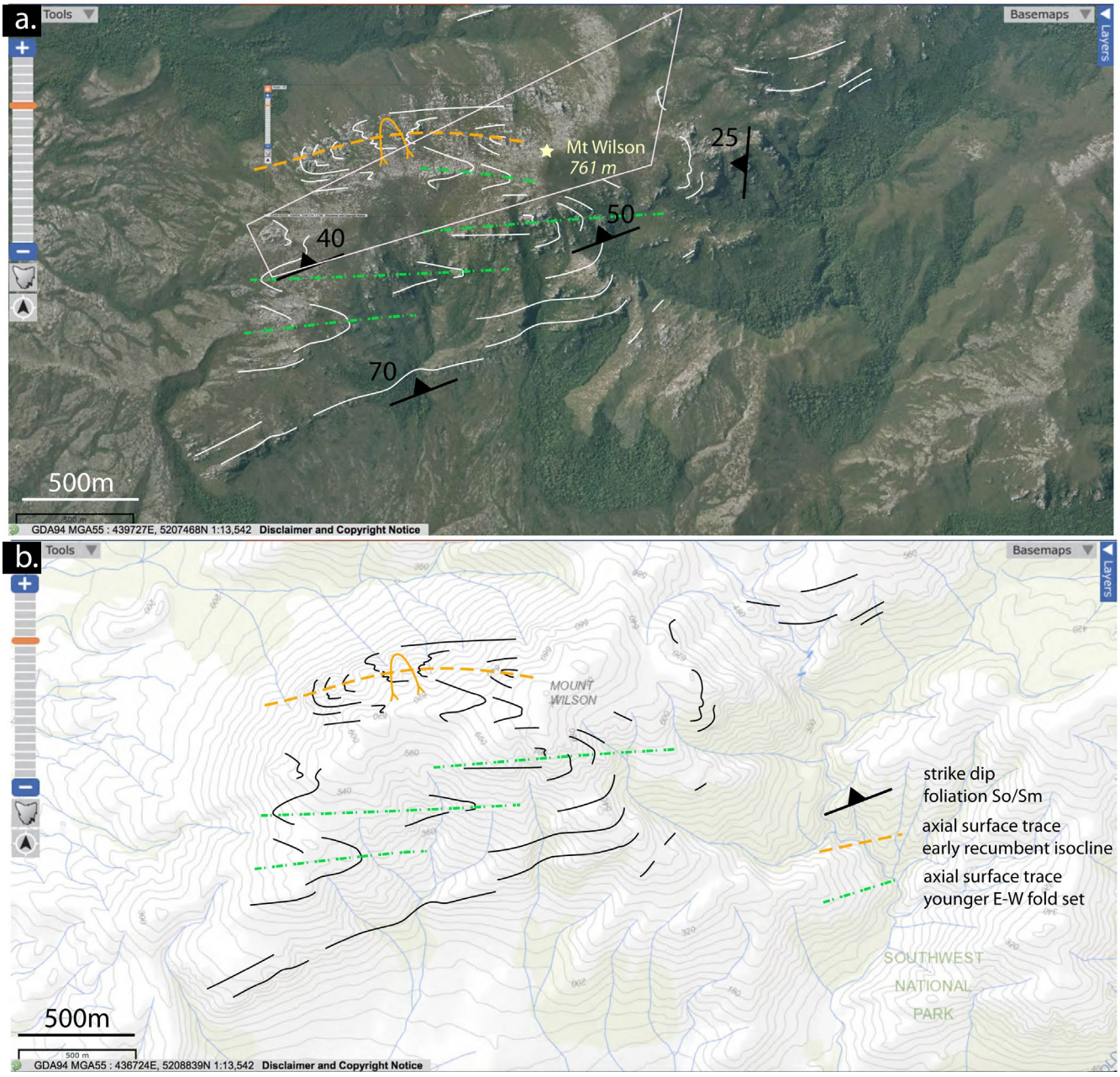

Figure 31. Mt Wilson structure map showing formlines in So/Sm (white line traces) interpreted from the ListMap air photo in a) and superimposed as black line traces on the ListMap topographic map in b). Structural data are from the preliminary Bathurst sheet based on the 1965 BHP mapping (Hall, 1965). The white polygon in (a) represents the projection of the Mt Wilson photo view shown in Figure 7.

Orange dashed line: recumbent fold axial surface trace; green dashed lines: open east-west fold axial surface traces.

4.5. Mount Norold

The Mt Norold ridgeline shows the recumbent fold couple refolded by several east-west trending open folds (dashed green lines as axial surface traces) (Figures 32 and 33). At the position of Mt Norold the folds have reclined geometry (Figures 33b, c, d and e). The fold pair is exposed in the northwest face of Mt Norold (Figure 34).

The northern face of the Mt Wilson-Mt Norold ridgeline (Figure 27, top right corner) shows another hillside intersection of the asymmetric folds (Figures 35 and 36). The regional position of this fold pair is shown in the northern end of Profile A-B (Figure 19) and the southern end of Profile C-D (Figure 19), where a fault is required to bring the fold pairs from this exposure to the same structural level as the pair exposed at Mt Norold.

Younger northwest-southeast trending fold axial surface traces refold a regional scale, recumbent isoclinal fold exposed in the northern face of the ridge (Figure 35).

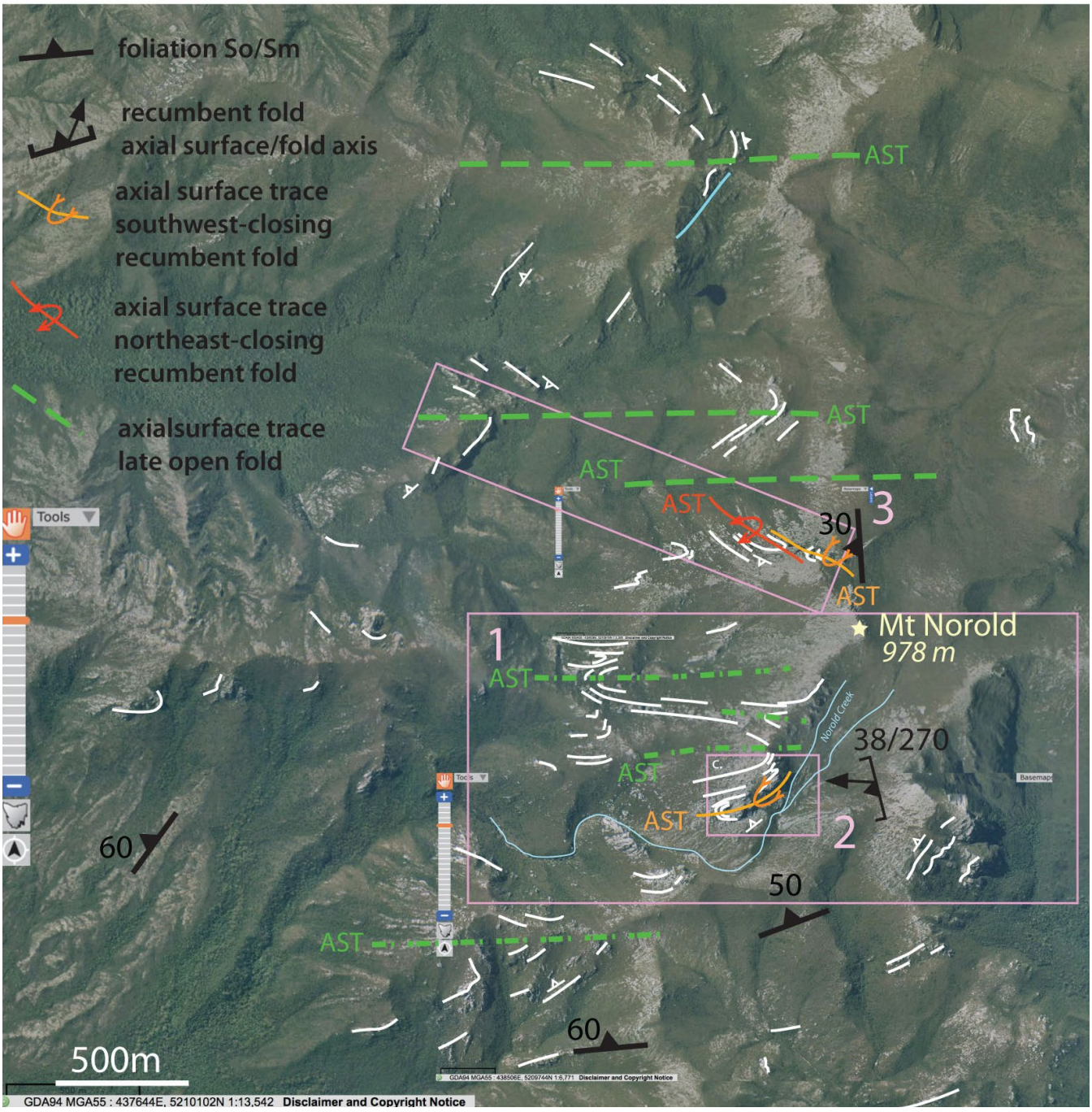

Figure 32: Structure map of the Mt Norold region north of the Old River valley on a ListMap satellite base. The positions of more detailed map areas 1 (Figure 33b), 2 (Figure 33c) and 3 (Figure 35) are shown by the pink-outlined rectangles.

White lines: formlines in So/Sm. Orange dashed lines: south-closing macro isocinal fold axial surface trace. Red dashed lines: north-closing macro isoclinal fold axial surface trace. Green dashed lines: east-west trending open, younger fold axial surface traces. Blue lines; brittle fault traces.

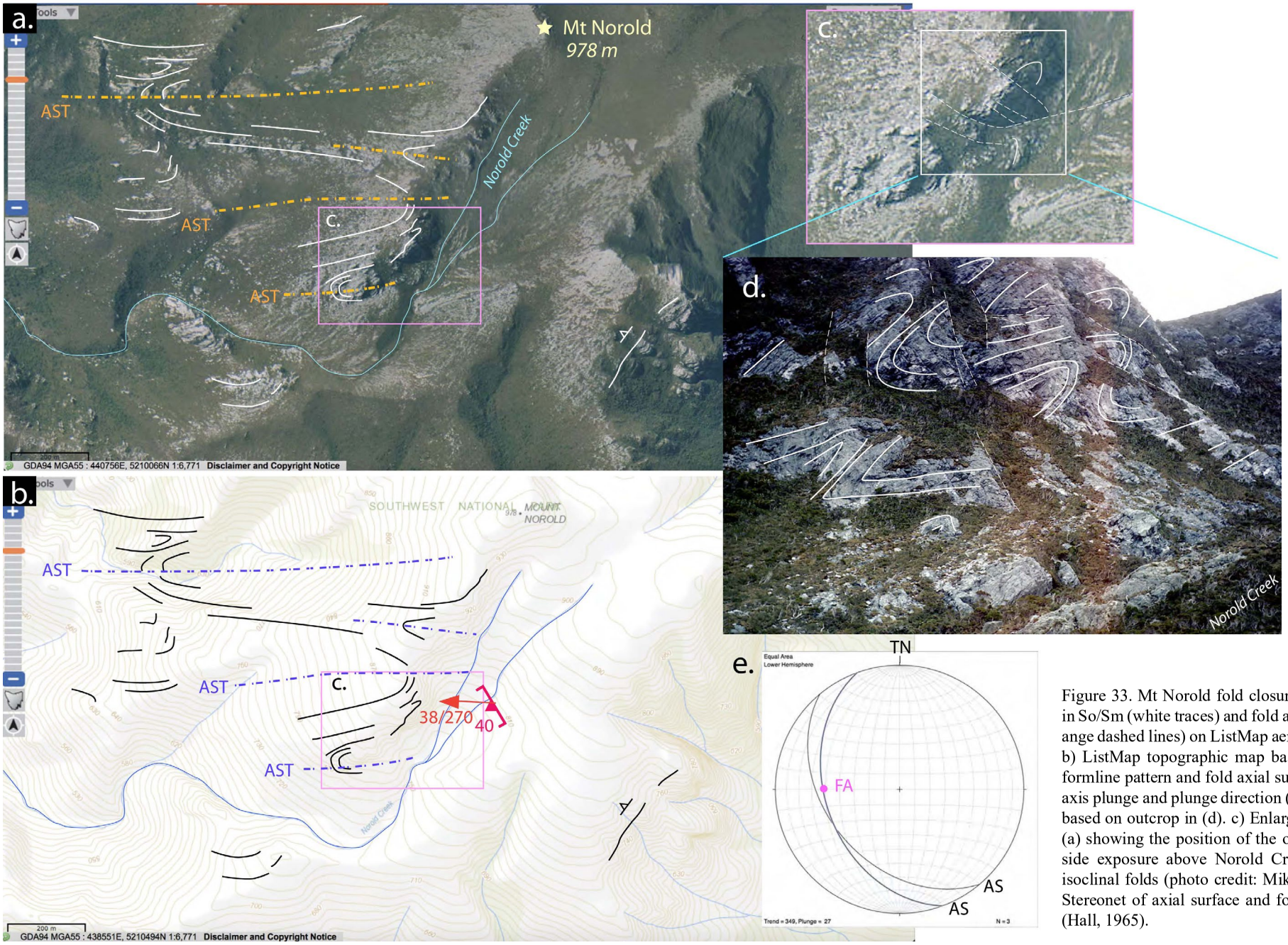

Figure 33. Mt Norold fold closures. a) Formline traces in So/Sm (white traces) and fold axial surface traces (orange dashed lines) on ListMap aerial photograph image. b) ListMap topographic map base with superimposed formline pattern and fold axial surface attitude and fold axis plunge and plunge direction (red dip/strike symbol) based on outcrop in (d). c) Enlargement of air photo in (a) showing the position of the outcrop in (d). d) Hillside exposure above Norold Creek showing reclined isoclinal folds (photo credit: Mike Hall circa 1965). e) Stereonet of axial surface and fold axis measurements (Hall, 1965).

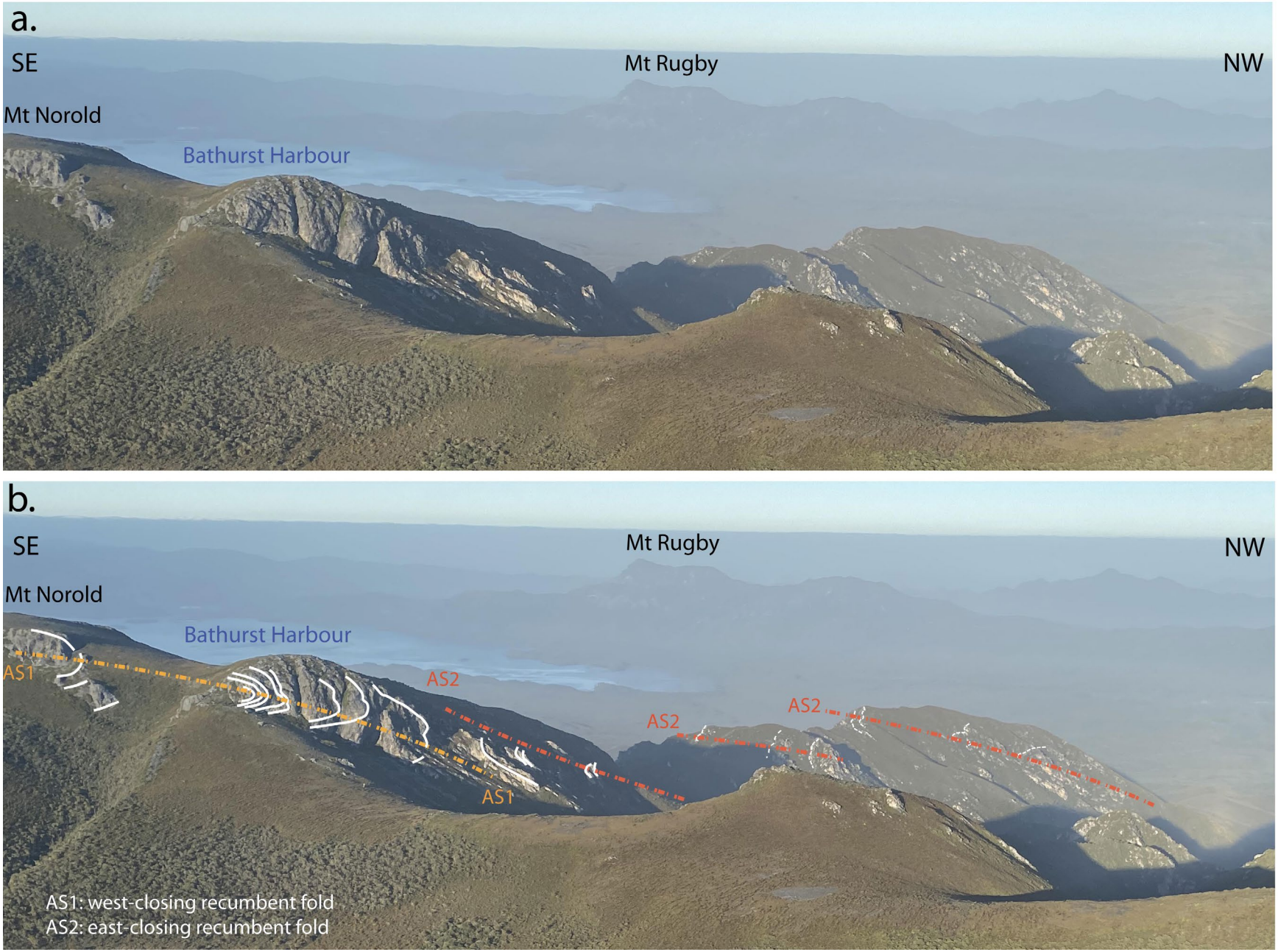

Figure 34. Northwest face of Mt Norold showing a west-closing recumbent fold (photo-left) sitting beneath a structurally higher, east-closing recumbent fold (middle to photo-right). Orange dashed line trace: southwest closing isoclinal macro-fold. Red dashed line trace: northeast closing isoclinal macro-fold.

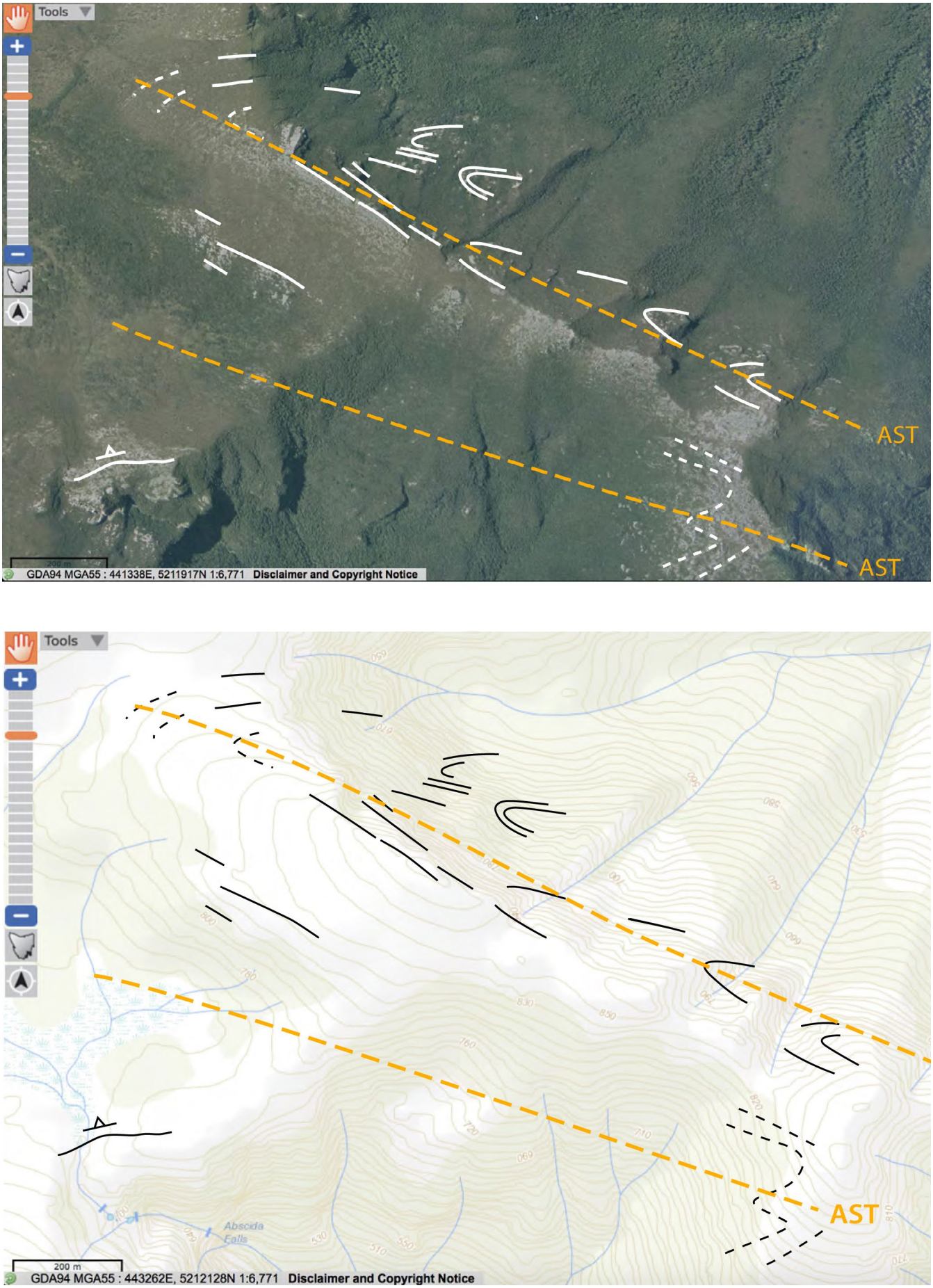

Figure 35. ListMap aerial photograph (a) and topographic map (b) of the ridgeline north of Mt Norold. Orange dashed lines: younger open fold axial surface traces.

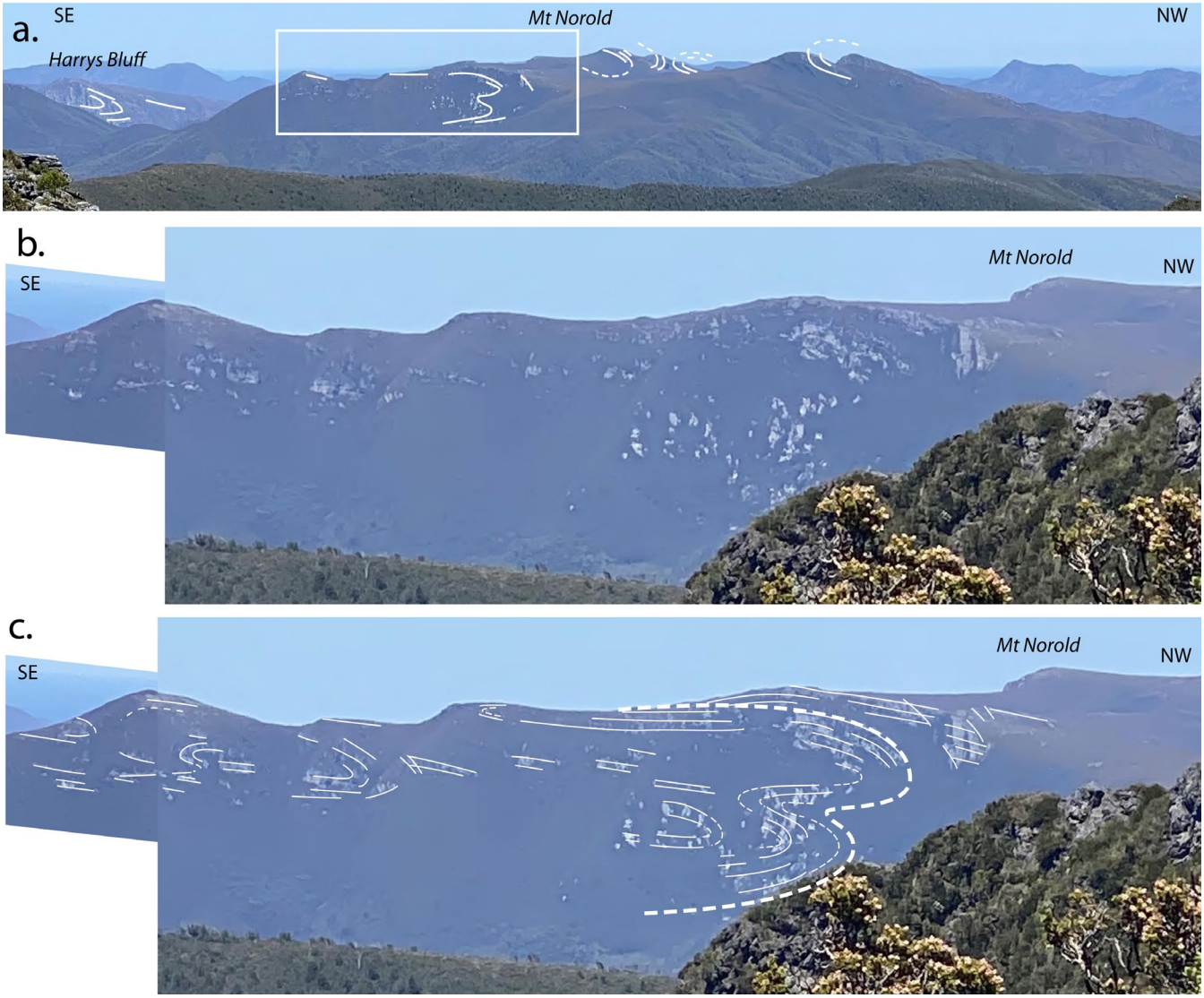

Figure 36. Ridge exposure to the north of Mt Norold showing discontinuous outcrop traces in quartzite defining apparent recumbent isoclinal fold closures. The oblique, non-profile view (potential hinge-parallel view) gives an apparent taper in the form of the macro-fold towards the southeast (left side of photo). a) Regional view to the south from Mt Aldebaran in the Western Arthur Range showing Harrys Bluff and Mt Norold. The enlarged ridge segment photograph in (b) is highlighted by the white rectangle. c) Interpreted So/Sm formline traces (white lines) in hillside shown in (b).

4.6 Crossing Gorge

The north-south trending cliff section of the Crossing River Gorge (Figure 3 top left corner of map and Figure 37a) shows a recumbent isoclinal macro-fold pair (Figures 37b, c and 38). The fold-pair consists of a structurally higher, south-closing fold hinge and a lower north-closing hinge. A series of north-dipping thrust and reverse faults truncate, juxtapose and repeat the fold-pair across the cliff section (Figure 37a and b). Both fold hinges can be seen in the northern portion of the cliff, but the hinges are juxtaposed by a listric-thrust fault with splays (Figure 37c). The middle and south portions of the cliff show fault repetition of the lower, north-closing recumbent fold hinge (Figure 37c).

The fault traces on the map (Figure 37b) show a major, more continuous lower fault with a series of splays that link or are truncated by this sole fault.

4.7 Maatsuyker Island Group

Offshore islands made up of metamorphosed Proterozoic rocks include the Maatsuyker Group of Maatsuyker Island, Walker Island and the Needles (Figures 39) consisting of a homoclinal, predominantly west-dipping sequence of highly deformed, grey, mica-schist (Pemberton, 1990; Banks, 1993) (Figures 40, 41 42 and 43). These include quartz-muscovite schist and quartz-chlorite schist with transposed So/Sm (ribbon schist), and minor porphyroblastic albite-schist (Banks, 1993).

This preliminary structural interpretation of the Maatsuyker group of islands is based on 1) description and limited structural data collected by Banks (1993), and 2) observations of foliation attitudes from Google Earth and photographs from the air and water. These data show that Walker Island, Maatsuyker Island and the Needles are part of a broad west-plunging synform with box-like form (Figure 39).

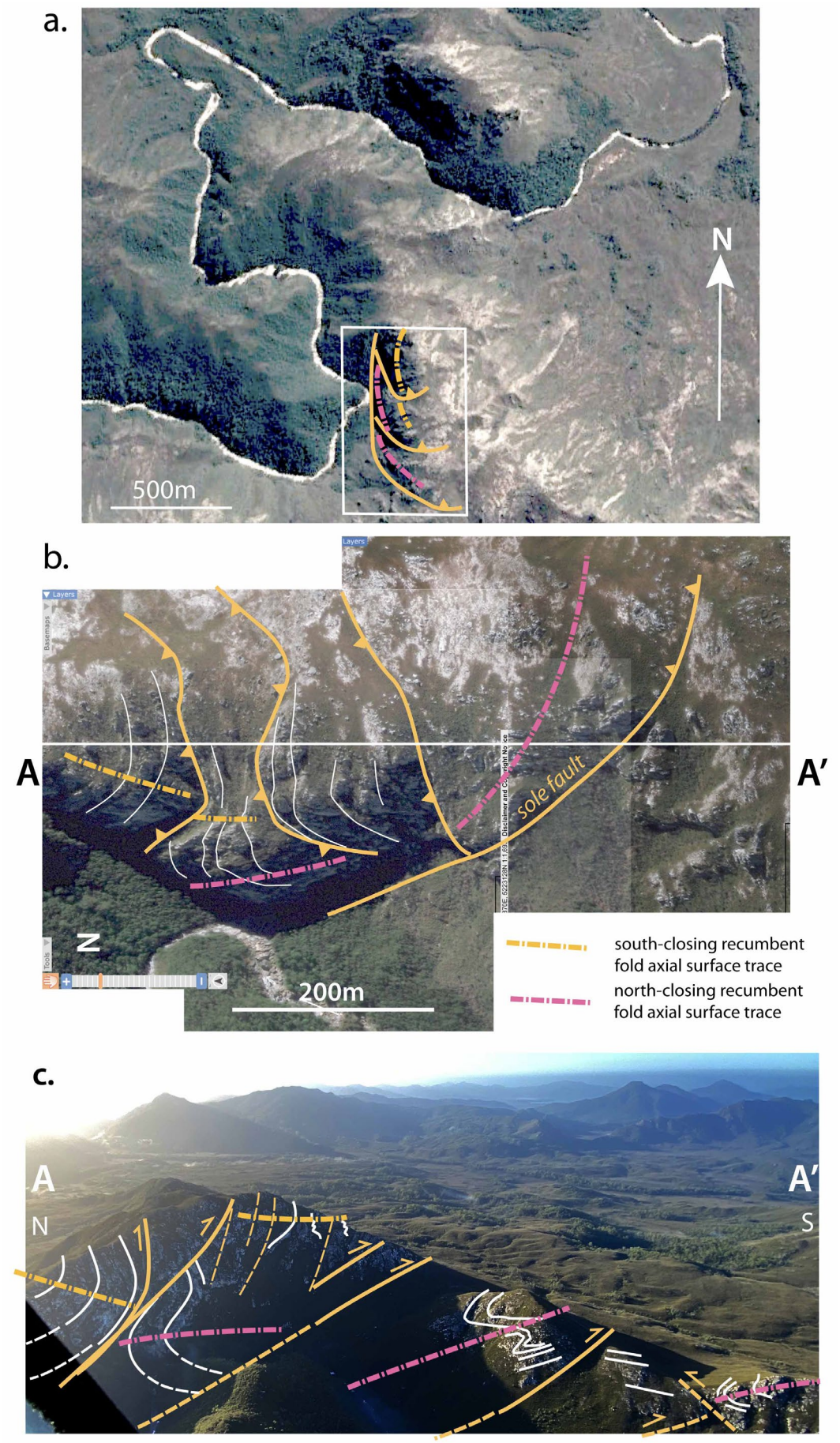

Figure 37. Structure of the Crossing River Gorge (GDA94, MGA55 425780E, 5223200N). a) Google Satellite image showing the Crossing River and the position of the Crossing River Gorge enlargement shown in (b). b) Structure interpretation map of part of the Crossing River Gorge showing formlines in So/Sm (white line traces) and reverse faults (orange line traces). Base is enlarged Google satellite image. The position of the photo profile A-A' is shown. Note the map is turned with north to the left. c) Aerial view of the cliff section of Crossing River Gorge. View is looking to the east.

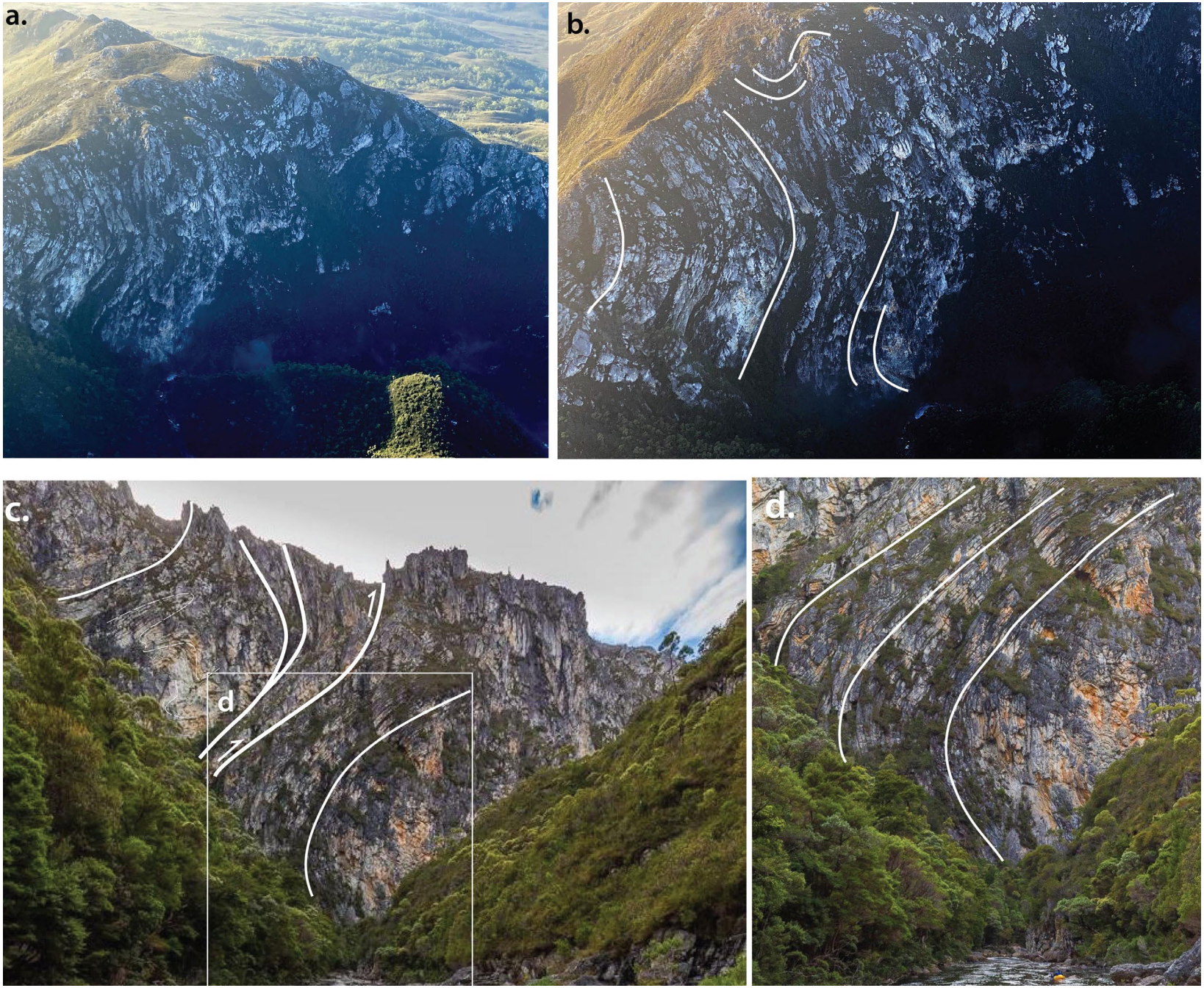

Figure 38. Photographs of the Crossing River Gorge recumbent, isoclinal macro-folds exposed in the cliffs above the gorge. a) Oblique aerial view from helicopter of the top part of the cliff section and ridge-line showing the south-closing hinge. b) Enlarged part of the cliff section showing parts of the two juxtaposed fold hinges. c) River level-view of the fold pair showing a series of north-dipping, curved (listric) thrust faults separating and juxtaposing the upper south-closing hinge against the lower north-closing hinge. The lower hinge is best seen at the river level as shown in (d). The river level photos (c) and (d) are by Grant Dixon.

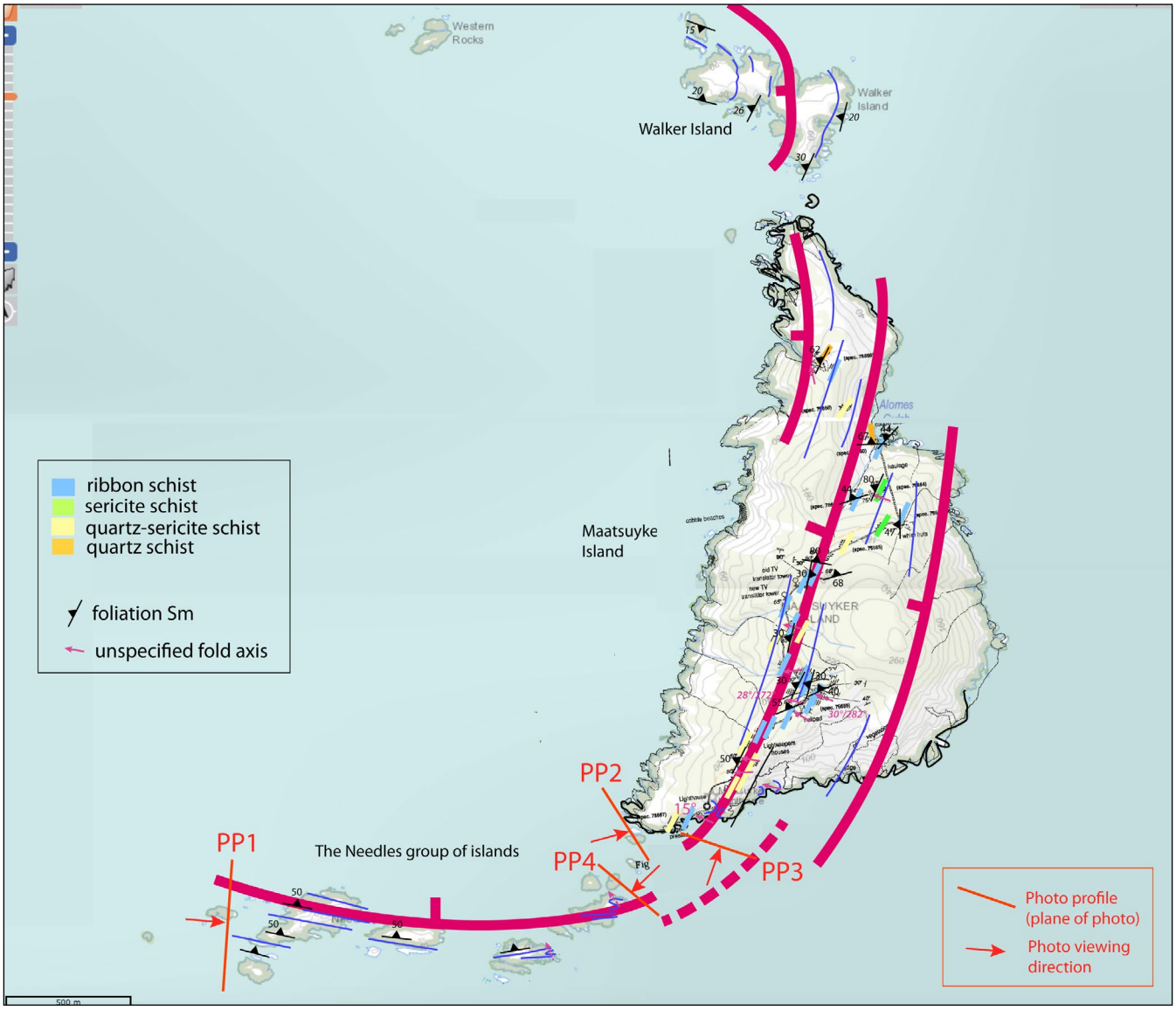

Figure 39 (above). Structure-lithology map of the Maatsuyker group of islands based on data from Banks (1993) and interpretation of Google Earth, ListMap airphotos and scenic photographs. The predominant layering lithology is ribbon schist (blue) and quartz-sericite schist (yellow).

Figure 40 (left). Aerial view along the Needles leading back to Maatsuyker Island (top left). The east-west trending Needles group-of-islands show moderately (~50°) north-dipping foliation Sm with transposed quartzite layers, quartz-mica schist and mica schist. Photo profile PP1 (for location see Figure 39). These islands define the southern limb of the broad, box-like, open, west-plunging Maatsuyker synvline. (Photo credit: Robyn Mundy, wrtingthewild.net)

Structure includes:

1. Sub-parallel schistosity Sm and transposed compositional layering So/Sm of quartz-mica and chlorite in schist.
2. Northwest-plunging, isoclinal macro-folds within So/Sm visible in the cliffs below the Maatsuyker Lighthouse at the south end of the island (Figures 41, 42 and 43).
3. Crenulations and mesoscopic folds with axial surface crenulation cleavage (fig.5, Banks, 1993) that are most likely associated with the east-trending, island-scale, box-like synform.
4. Brittle faults that truncate and offset the macro-folds and the foliation Sm (Figures 42 and 43b).

Structural measurements by Banks (1993) show:

1. Poles to compositional layering defining a weak great circle with modal dip of ~43° towards ~300°
2. Plunge data from 18 mesoscopic folds and crenulations give a modal attitude of 45°-50° towards ~300°.

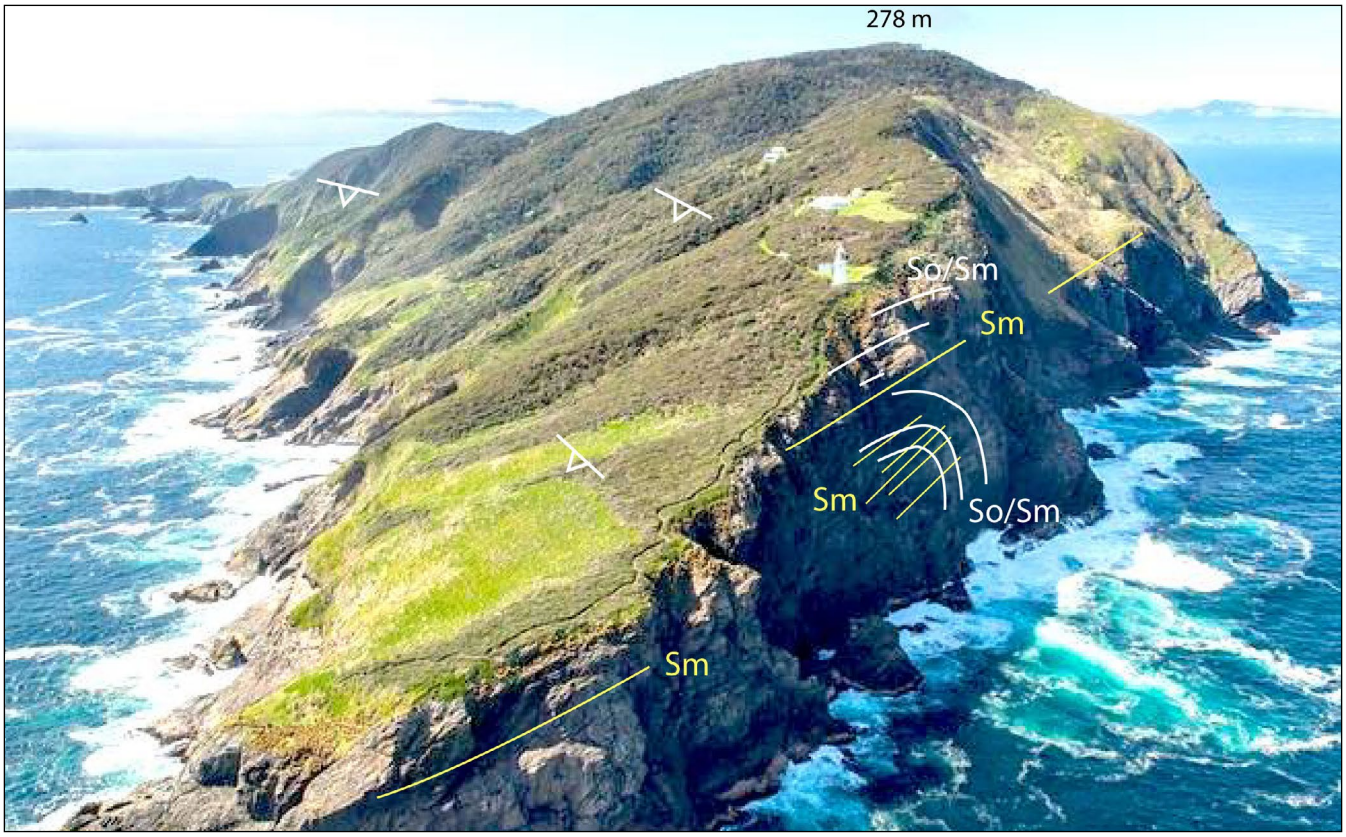

Figure 41 (above). Aerial view looking northeast along the Maatsuyker Island ridgeline showing the pronounced dip slope on the grassed western side dictated by the schistosity in the interlayered ribbon schist, quartz schist and quartz-sericite schist. Photo profile PP2 (for location see Figure 39). (Photo credit: Amanda Walker)

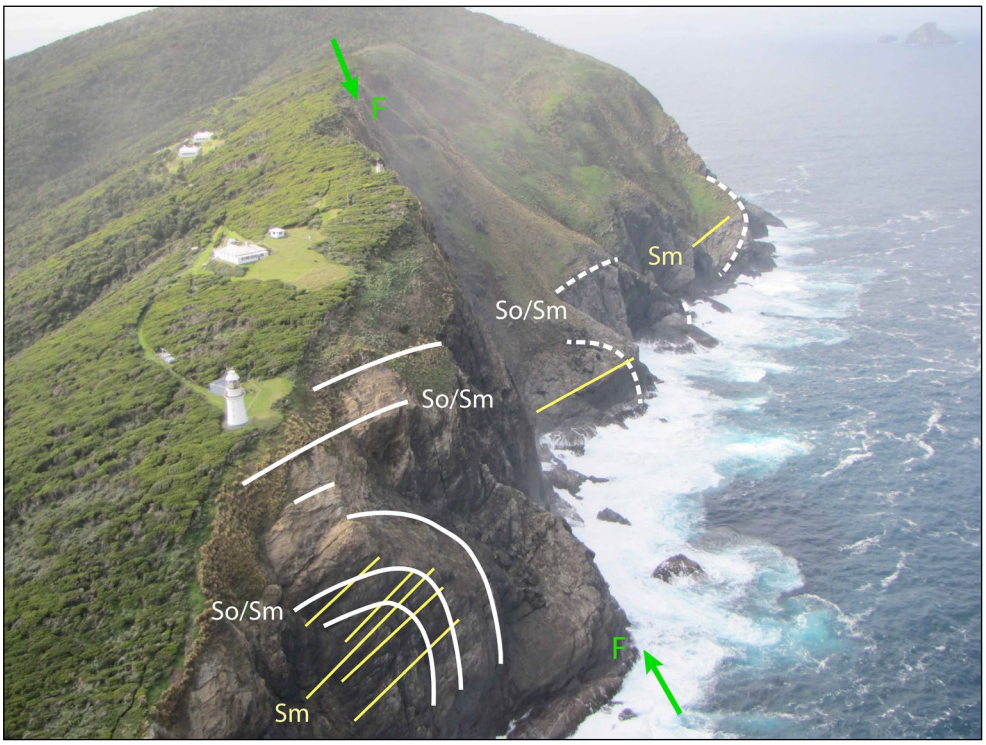

Figure 42 (right). Aerial view of Maatsuyker lighthouse with intense, west-dipping foliation Sm dominating the sea cliffs and defining the pronounced western-flank dip slope of the island (compare with Figure 41). The centre of the photo shows the cliffline cut by a 60° southeast dipping fault shown by the green trace (compare with Figure 43b). Photo profile PP3 (for location see Figure 39). (Photo credit: Wildcare Tasmania)

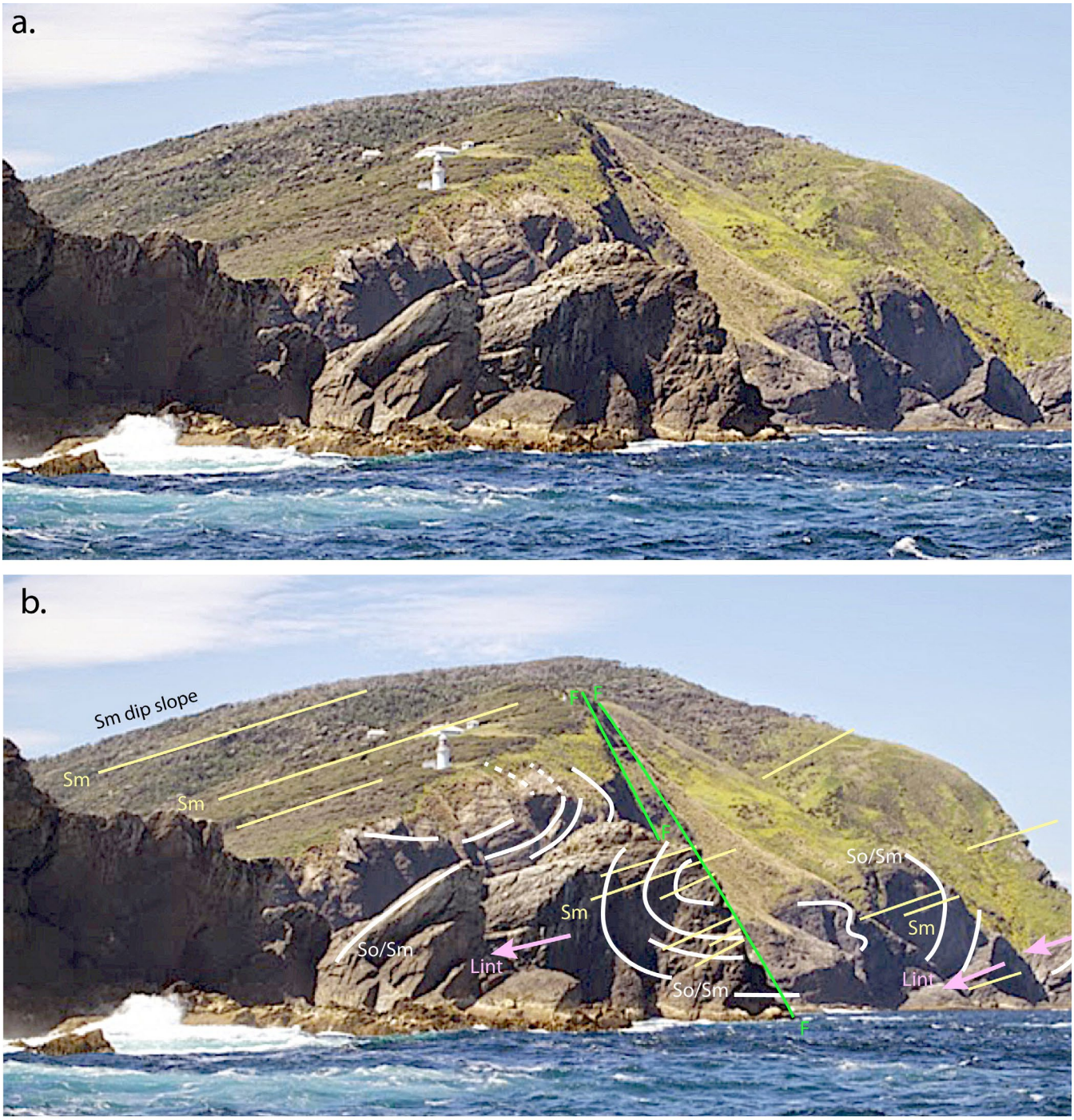

Figure 43. Sea-level view of the south end of Maatsuyker Island with the Lighthouse visible (centre left of photo). A northwest-plunging, macro-isoclinal fold-pair sit in the cliffs below the Lighthouse. These are cut by the fault (green line trace) with apparent normal-sense movement (compare with Figure 42). Photo profile PP4 (for location see Figure 39). (Photo credit: Annalise Rees) *white line traces: compositional layering So/Sm; yellow line traces: foliation Sm; green line traces: faults; pink arrows: intersection traces of Sm or the equivalent macro-fold axis plunges.*

5.0 IMPLICATIONS OF THE MACRO-FOLD PAIR IN THE EASTERN SOUTHERN TYENNAN

The eastern Southern Tyennan fold-pair distribution and geometry matches a fold "wave" train as a fold system of consistent and repeated S-vergent asymmetric fold pairs at the same structural level (Figure 44). This geometry is supported by structural profile construction (Figure 19) where spatially isolated fold hinges can be assembled and constrained as a wave train within the fold pair. The folds do not appear as isolated fold pairs at different levels, although they do fold all units in the litho-tectonic stack (Figure 44a).

Dimensions of the asymmetric fold-pairs are best shown by 1) the fold-pair upper limb to fold-pair lower limb perpendicular distance (limb separation distance or fold wavelength equivalent) and 2) the hinge separation distance (Figure 45a).

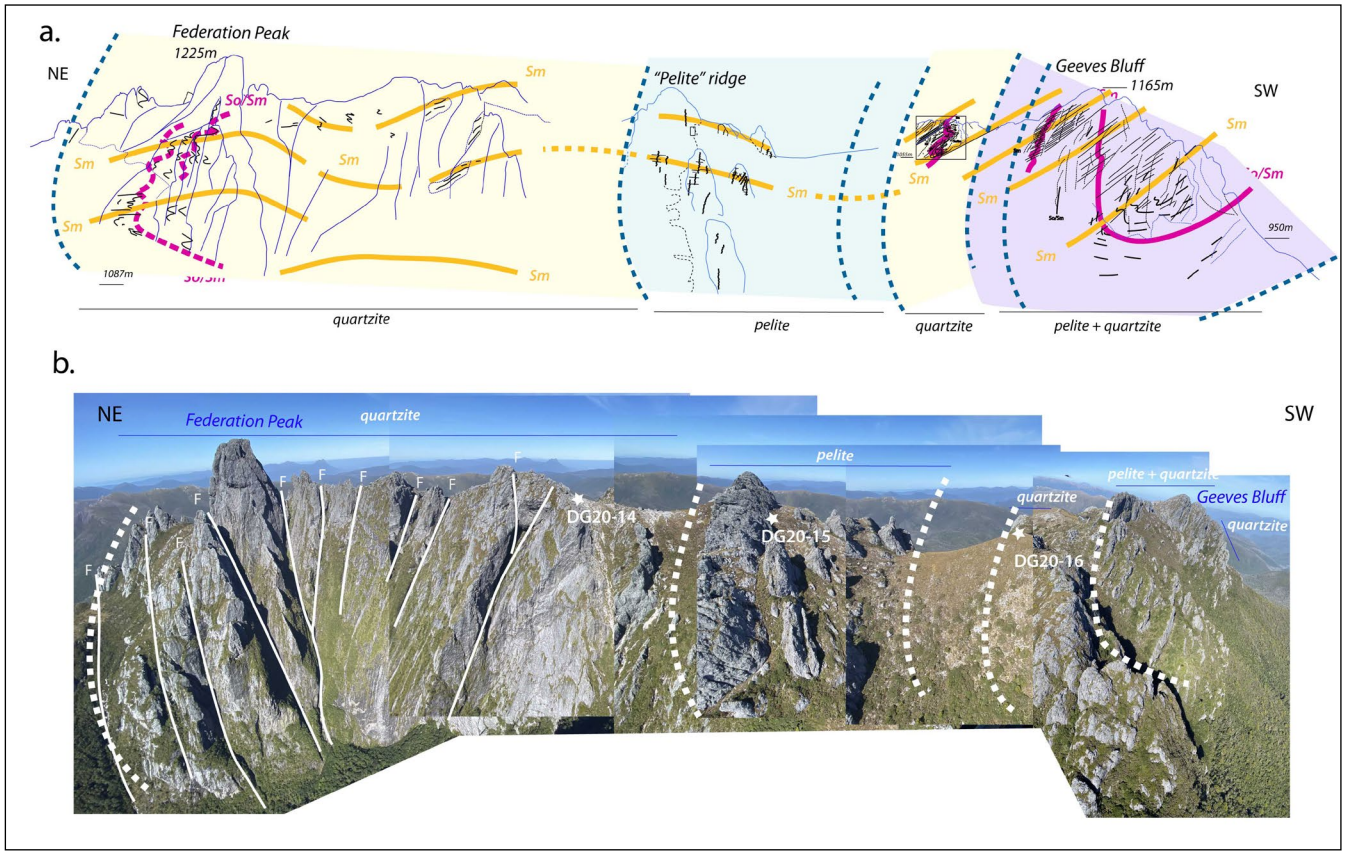

Figure 44. Example of layers or litho-tectonic units folded through a macro-isoclinal fold hinge in the eastern Southern Tyennan domain. a) Federation Peak-Geeves Bluff structural profile with So/Sm formlines (black line traces), layer contacts (blue dashed line traces), axial surface foliation Sm formlines (orange and orange dashed line traces). Lithologies are quartzite (yellow), pelite (light blue) and mixed pelite and quartzite (light mauve). b) Photo collage of Federation Peak-Geeves Bluff ridgeline used to construct the structural profile shown in (a).

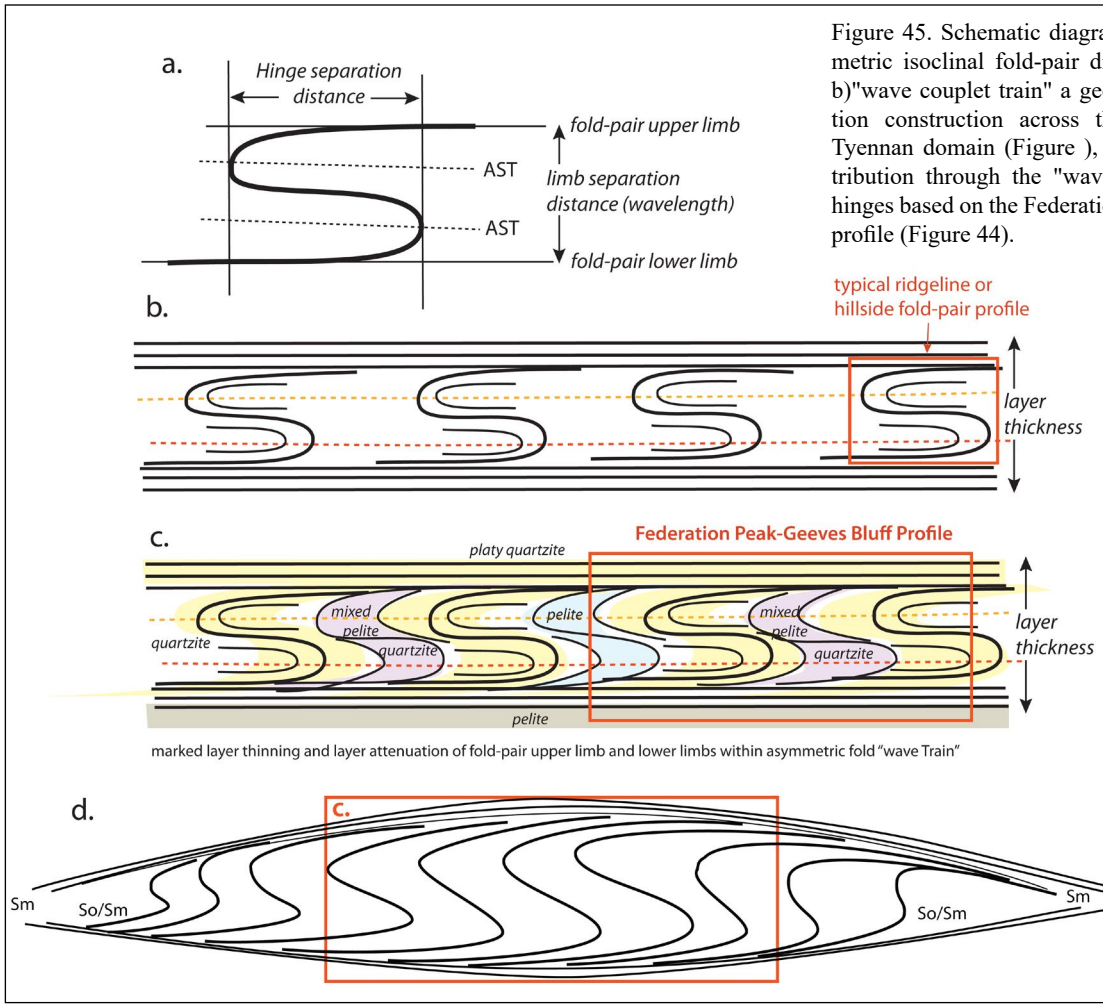

Figure 45. Schematic diagram showing a) asymmetric isoclinal fold-pair dimension parameters, b)"wave couplet train" a geometry based on section construction across the eastern Southern Tyennan domain (Figure), and c) lithology distribution through the "wave couplet train" fold hinges based on the Federation Peak-Geeves Bluff profile (Figure 44).

- Determinations of the limb separation distance (LSD) gives a ~430 m distance, for three localities including Harrys Bluff (~430 m), Mt Castor (~430 m) and Mt Pollux (~425 m).
- Determination of the fold-pair hinge separation distance (HSD) was problematical due to the obliquity of most of the photos with respect to the fold hingelines. There is a suggestion however that the HSD dimension is approximately equal to the limb separation distance (LSD), namely ~400-450 m.
- Estimates from the Harrys Bluff cliff exposure suggest the quartzite has ~700 m thickness.
- This fold pattern extends across an area of ~60 km length and ~20 km width, approximately 1200 km^2 (Figures 3 and 4).

Development of such an asymmetrical fold-pair with the form shown in Figure 45b is geometrically suggestive of a major, regional-scale shear lozenge cored by asymmetric folds (Figure 45d). The evolution of this basal regional shear "zone" on the lower limb of the South West Cape mega-sheath fold requires 1) initial imbricate stacking of the lithotectonic units in this basal zone with unit repetition as a duplex zone (Figure 45c), and 2) large shear strain across the extent of the eastern Southern Tyennan domain (Figure 45d).

A possible fold evolution analogy is that of a rug on a table, where the trailing part of the rug "catches up" with an essentially "pinned" or slower moving leading edge, as a fold "wave train" of wrinkles (folds) develops at the rear. The analogy implies a subtle timing difference between the mega-sheath fold development and the lower-limb fold-wave train with the "wave train" development largely post the mega-sheath fold.

6.0 ACKNOWLEDGMENTS

- Mineral Resources Tasmania (Andrew McNeill) for providing support through the 2016-2020 Geoscience Initiative.
- Chris Large for editing and formatting this Tasmanian Geological Survey publication.
- Parks and Wildlife Service (PWS) for allowing helicopter access and landing in the World Heritage Area as well as permits for measurement, sampling and photograph collection.
- Jason Bradbury NRE (Department of Natural Resources and Environment) for assistance with WHA and PWS permits for scientific research.
- Rodney Smith from Rotorlift for helicopter transport into the Tasmanian southwest.
- Rick Allmendinger and Nestor Cardozzo for use of OSX Stereonet.

7.0 REFERENCES

Banks, M.R. 1993. Reconnaissance Geology and Geomorphology of the Major Islands South of Tasmania. Unpublished Report. Tasmanian Department of Parks, Wildlife and Heritage, 65p.

Corbett, K. D. and Vicary, M. J., 2014. Chapter 4.5, Middle Cambrian Post-Collisional Volcanism, In Corbett, K. D., Quilty, P.G. and Calver, C. R., eds, *Geological Evolution of Tasmania*, pp 145-183. Geological Society of Australia Special Publication, 24, Geological Society of Austrlaia (Tasmania Division).

Gray, D.R. and Vicary, M. J., 2021a. Structural Geology of Frenchmans Cap, Central Tyennan Domain, Tasmania. Mineral Resources Tasmania, *Geological Survey Paper,* 6, 44p.

Gray, D.R. and Vicary, M. J., 2021b. Structural Geology of the Central Tyennan Region, Tasmania. Mineral Resources Tasmania, *Geological Survey Paper,* 7, 69p.

Gray, D.R. and Vicary, M. J., 2022a. Structural Geology of the Arthur Range, Central Tyennan Domain, Tasmania. Mineral Resources Tasmania, *Geological Survey Paper,* 8, 79p.

Gray, D.R. and Vicary, M. J., 2022b. Mega-Sheath Fold Core of the Southern Tyennan Domain, Tasmania: The De Witt-Propsting and South West Cape Sheath Fold Systems. *Geological Survey Paper*, 10, 80p.

Gray, D.R. and Vicary, M. J., 2022c. Structural Geology of the Red Point Macro-fold, *Geological Survey Paper*, 12, in press.

Gray, D.R. and Vicary, M. J., 2022d. A Structural Synthesis of the Southern Tyennan Domain, southwest Tasmania. *Geological Survey Paper*, 13, in press.

Gray, D.R., Vicary, M. J. and McNeill, A.W., 2022. Structure of the High-grade Coastal Belt, Southern Tyennan Domain, Tasmania. Mineral Resources Tasmania, *Geological Survey Paper*, 9.

Hall, W.D.M. 1965. Unpublished Progress Report No.1-March-June 1965 for Exploration Licence 13/65 Southwest Tasmania: Geological and geochemical exploration in the area between Bathurst Channel, Cox Bight and South West Cape. 68p. TCR 65-0398.

Lennox, P.G., 2013. Geology of parts of the Bathurst and Maatsuyker map sheets. Tasmanian Geological Survey Record 2013/03, 30p.

Mulder, J.A., 2013. The Structure and Metamorphism of the Cox Bight-Red Point Area, South West Tasmania. Unpublished Honours Thesis, The University of Tasmania. 76p.

Mulder, J.A., Berry, R.F. and Scott, R.J., 2015. The structure and metamorphism of the Red Point Metamnoirpohic Complex-- A newly discovered high-pressure metamorphic complex from the south coast of Tasmasnia. *Australian Journal of Earth Sciences*, 62, 969-983.

Pemberton, M., 1990. Aspects of the Soils, Geomorphology and Geology of Maatsuyker Island, Tasmanian Department of Parks, Wildlife and Heritage, Unpublished Report.

Ramsay, J.G. 1967. *The Folding and Fracturing of Rocks*. McGraw Hill.

Stefanski, M.Z. 1957a. Progress Report on Regional Geological Survey of the Port Davey-Cox Bight Area. *Tasmanian Department of Mines Technical Report,* 2, p.87-106.

Stefanski, M.Z. 1957b. Geological Compilation in the Bathurst Harbour Area. Unpublished Map, Mineral Resources Tasmania.

Taylor, A.M., 1959. Precambrian Rocks of the Old River Area. Tasmanian *Geological Survey Technical Report*, 4, p.34-36.

Williams, P.R. 1979. Basin Development, Environment of Deposition and Deformation of a Precambrian? Conglomeratic Flysch Sequence at Bathurst Harbour, SW Tasmania. Unpublished PhD Thesis, The University of Tasmania.

Tasmanian
Government

Mineral Resources Tasmania
PO Box 56 Rosny Park
Tasmania Australia 7018
Ph: +61 3 6165 4800

info@mrt.tas.gov.au www.mrt.tas.gov.au